MARMARA UNIVERSITY

FACULTY OF ENGINEERING

THERMODYNAMIC ANALYSIS AND OPTIMIZATION OF HEAT PUMPS USING CO_2 AS THE WORKING FLUID

Hüseyin Kaya , Sercan Başar

Müdek Final Project Commission			
The essential features of an acceptable design Project			
		Satisfied	Unsatisfied
1	Mechanical or Thermal Design	✓	
2	Report writing technique	✓	
3	Development of student creativity		☑
4	Use of open-ended problems		☑
5	Formation of design	✓	
6	Problem statement and specification	✓	
7	Synthesis of alternative solutions		☑
8	Feasibility	✓	
9	Detailed system description	✓	
10	Consideration of constraints (e.g. economic, safety, reliability, etc.)		☑
11	Utilization of engineering and scientific principle	✓	
Decision		Signature	
Accepted but not approved		19.07.2021	
Prof. Dr. Bülent Ekici,		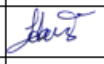	
Dr. Öğr. Üyesi Uğur Tümerdem			
Ar. Gör Serkan Öğüt			

GRADUATION PROJECT REPORT

Department of Mechanical Engineering

Supervisor

Doç. Dr. Barış Yılmaz

ISTANBUL, 2021

MARMARA UNIVERSITY

FACULTY OF ENGINEERING

THERMODYNAMIC ANALYSIS OF CO_2 HEAT PUMPS

by

Hüseyin Kaya, Sercan Başar

January,2021 ,Istanbul

SUBMITTED TO THE DEPARTMENT OF MECHANICAL ENGINEERING IN PARTIAL FULFILLMENT OF THE REQUIREMENTS FOR THE DEGREE OF

BACHELOR OF SCIENCE

AT

MARMARA UNIVERSITY

Signature of Author(s) ..... Sercan Başar Hüseyin Kaya

Department of Mechanical Engineering

Certified By ..... Doç. Dr. Barış YILMAZ

Project Supervisor, Department of Mechanical Engineering

Accepted By ..... Prof Dr Bülent EKICI .....

Head of the Department of Mechanical Engineering

ACKNOWLEDGEMENT

First of all, we are grateful to our supervisor Assoc. Prof. Barış Yılmaz, who helped in getting this project done and through out the lesson, brought us up to this stage. We feel there words are not enough to express how much thankful to him.
We would like to thank TÜBİTAK for supporting this study within the scope of the University Students Research Projects Support Program.

July,2021 Sercan Başar, Hüseyin Kaya

CONTENTS

ACKNOWLEDGEMENT i

ABBREVIATIONS iv

SYMBOLS v

ABSTRACT vi

LIST OF FIGURES vii

LIST OF TABLES ix

1.INTRODUCTION 1

1.1.Literature Review 2

1.2.The History of R744(CO_2) 2

1.3.Carbon Dioxide (R744-CO_2) Properties 3

1.4.The Comparison of CO_2 with Other Refrigerants 5

1.5.CO_2 Heat Pumps Usage Areas 7

1.5.1.Vending machines and bottle coolers 7

1.6.Transcritical CO_2 Heat Pump System And Comparison With Conventional Subcritical Vapor Compression System 9

1.7.Components of Transcritical R744 Heat Pumps 10

1.7.1.Compressors 10

1.7.2.Throttling Valves 11

1.7.3.Evaporators 12

1.7.4.Gas Cooler 13

1.7.5.Internal Heat Exchangers(IHX) 13

1.7.6.Flash Tank 13

1.8. Alternative Systems of CO_2 Heat Pumps 14

1.8.1. Heating Demand in Residential Buildings 14

1.8.2. Residential Basic Transcritical CO_2 Heat Pumps Systems(BTS) 15

1.8.3. Basic Two-Stage Cycle (BTC) with Two Compressors 16

1.8.4.An Ejector Enhanced Sub-Cooler Vapor Injection CO_2 Heat Pump Cycle (ESCVI) 17
1.8.5. Two-Stage Transcritical CO_2 Heat Pump Cycle with Double Ejectors (ETC) 18
2.METHODOLOGY 20
2.1.Thermodynamic Analysis of CO_2 Heat Pumps Components 20
2.1.1.Compressor 21
2.1.2Throttling Valves 21
2.1.3.Evaporator 21
2.1.4.Gas Cooler 22
2.1.5.Internal Heat Exchanger 22
2.1.6.Flash Tank 23
2.1.7.Ejector 23
3.RESULTS 26
3.1.Input Data and Assumptions For CO_2 Heat Pump With Internal Heat Exchanger 26
3.2.Results of CO_2 Heat Pump With Internal Heat Exchanger 27
3.3.Results of CO_2 Heat Pump on BTC Cycle with Two Compressors 31
3.4.Results of ESCVI System 36
3.5.Results of ETC System 45
4.OPTIMIZATION STUDIES 53
4.1. BTC Cycle 53
4.2.ESCVI Cycle 55
4.3.ETC Cycle 57
5.CONCLUSION 60
6.REFERENCES 61

ABBREVIATIONS

BTC: Basic Two-Stage Cycle with Two Compressors

BTS: Basic Transcritical CO2 Heat Pump System

CFC: Chlorofluorocarbon

DHW: Domestic Heat Water

EES: Engineering Equation Solver

ESCVI: Single Ejector Advanced Supercooler Steam Injection CO2 Heat Pump Cycle

ETC: Dual Ejector Two Stage Transcritical CO2 Heat Pump Cycle

eva: Evaporator

gc: Gas Cooler

HCFC: Hydrofluorocarbon

HP: High Pressure

IHX: Internal Heat Exchanger

LP: Low Pressure

SYMBOLS

P: Pressure

T: Temperature

h: Enthalpy

s: Entropy

W: Work

Q: Heat

φ: Isentropic Efficiency

$\dot{X}$: Exergy Lost

$\dot{W}$: Power

$\dot{m}$: Mass Flow Rate

μ : Entraintment Ratio

r_p : Pressure Lift Ratio

ΔT_{sub} : Sub-Cooling Degree

COP: Coefficient of Performance

u: Velocity of Fluid

ABSTRACT

In recent years, it has become important to use less fossil fuel-based combustion systems in order to reduce the effects of global climate change. With the increase in the importance of energy efficiency, the use of heat pump systems using natural resources in space heating and cooling is increasingly common. In addition, with the increase of environmental sensitivity, systems using natural fluids that do not damage the atmosphere and the ozone layer, have low global warming potential and have no ozone depletion potential are preferred. One of the fluids used in these systems is carbon dioxide. CO_2 is a fluid naturally found in the atmosphere, with a global warming potential of 1 (one), an ozone depletion potential of 0 (zero), and its use in heat pumps is increasing day by day. Carbon dioxide; It can be used in different systems depending on the external environment conditions including subcritical and transcritical. It is more advantageous to use transcritical systems in our country where average air temperature is high. In this study, thermodynamic analysis will be done to examine the energy performance of a heat pump with transcritical CO_2 fluid. For this purpose, energy and exergy analysis of the system alternatives determined as a result of the literature research will be done. If we list the system alternatives that we used; Residential Basic Transcritical CO_2 Heat Pump Systems and Residential CO_2 Heat Pump Systems with Integrated Tripartite GasCooler. These studies will be analyzed with EES (Engineering Equation Solver) and MATLAB Coolprop software, which is frequently used in such analyzes. Parametric analysis of selected systems will be made and their effects on energy efficiency will be examined.

The main purpose of this thesis is to observe the differences between different CO_2 refrigerated heat pump systems by making energy and exergy analyzes and to choose the most optimum system for us both in terms of economy and contribution to nature.

LIST OF FIGURES

Figure 1 - Comparison of Pressures of Different Types of Refrigerants[10] 4
Figure 2- Pressure-Enthalpy Diagram of R744[10] 5
Figure 3- R744 Cycle Components[10] 8
Figure 4- R744 Cooling Cassette[10] 8
Figure 5- Coca Cola Vending Machines[10] 9
Figure 6- A simple standard air compressor [14] 11
Figure 7-A simple throttling valve[15] 11
Figure 8 – A Standard Evaporator [15] 12
Figure 9- A Standard Gas Cooler [14] 13
Figure 10- A Standard Internal Heat Exchanger 13
Figure 11-Schematic of the Flash Tank 14
Figure 12- The Different Heating Demands In Single-Family Houses [9] 15
Figure 13-Basic CO_2 Heat Pump Water Heater [9] 16
Figure 14-The BTC cycle schematic system 17
Figure 15-The Schematic System of ESCVI Cycle 18
Figure 16-The Schematic System of ETC Cycle 19
Figure 17- Transcritical CO_2 Heat Pump with Internal Heat Exchanger [9] 20
Figure 18-Flow Chart for The Numerical Solution of CO_2 Heat Pump With Heat Exchanger 26
Figure 19- T-s diagram for CO_2 heat pump with internal heat exchanger cycle 27
Figure 20- P-h diagram for CO_2 heat pump with internal heat exchanger cycle 28
Figure 21- Graph for COP-Gas Cooler Outlet Temperature 29
Figure 22- Graph for COP-Evaporator Temperature 30
Figure 23- Component Based Exergy Lost Variation With Evaparator Temperature 30
Figure 24-T-s diagram for CO_2 heat pump on BTC cycle with two compressors 31
Figure 25-P-h diagram for CO_2 heat pump on BTC cycle with two compressors 32
Figure 26-Graph for COP-Evaporator Temperature 33
Figure 27-Graph for COP-High-side Pressure 34
Figure 28-Graph for COP-Sub Cooling Degree 35
Figure 29-Component Based Exergy Lost Variation With Gas Cooler Temperature 35
Figure 30- T-s Diagram of ESCVI Cycle 36
Figure 31- P-h Diagram of ESCVI Cycle 37

Figure 32- Graph for COP-High-side Pressure 38
Figure 33-The Effect of Discharge Pressure on Ejector System 39
Figure 34-Graph for COP-Evaporator Temperature 40
Figure 35-The Effect of Evaporator Temperature on Ejector Performance 41
Figure 36-The Effect of Ejector Efficiency 42
Figure 37-Graph for COP-Entrainment Ratio(μ) 43
Figure 38-Graph for COP-Pressure Lift Ratio(r_P) 44
Figure 39-The Effect of Evaporator Temperature on Exergy 45
Figure 40-Solving Procedure of The BTC Cycle 46
Figure 41-P-h Diagram of ETC Cycle 47
Figure 42-T-s Diagram of ETC Cycle 48
Figure 43-The Graph of COP-Ejector Efficiency 49
Figure 44-Graph of COP-Evaporator Temperature 50
Figure 45-Graph of The Effect of Evaporator Temperature on Ejector Performance 51
Figure 46-Graph of COP-High-side Pressure 52
Figure 47-Graph of The Effect of Gas Cooler Pressure on Ejector Performance 53

LIST OF TABLES

Table 1- General Properties of Carbon Dioxide 3
Table 2-Properties of Some Refrigerants 6
Table 3- Main Differences Between Trancritical and Subcritical R744 Heat Pump Cycle 10
Table 4- Comparison of Expansion Valves 12
Table 5- The High-side Pressure With Outlet Temperature of Water 28

1.INTRODUCTION

Economic activities that took place in the triangle of industrialization, growth and development led by the developed countries throughout the 20th century resulted in a pollution that the environmental areas where people live cannot bear. Soil, water and air are faced with a level of pollution that threatens human life. Countries that have started to realize the dimensions of the problem have sought a permanent solution [1]. New standards and norms are developed and implemented in this field every year. The companies associated with the process also have to develop technologies, products and manufacturing (process) methods in accordance with new laws and standards in order to adapt to the developments.

Like many branches of industry, the air conditioning sector is also affected by these developments. Studies are carried out to find environmentally compatible refrigerant solutions instead of chlorofluorocarbons (CFC) and hydrochlorofluorocarbons (HCFC), which are used in cooling systems, accelerate global warming, harm the ozone layer and have a negative effect on the environment. Hydrofluorocarbons (HFC) are synthesized from natural gases such as ethane and methane, which do not contain chlorine, and hydrogen is substituted for chlorine and therefore they are defined as relatively environmentally friendly [2, 3]. In addition to CO_2, natural fluids such as isobutane and propane cannot be used in systems with large charge because they are flammable and explosive. The effects of R717 (NH3, Ammonia) gas on copper alloys and the risk of poisoning in collective spaces and systems with large charge emerge as disadvantages.

Natural refrigerants that do not affect global warming and do not damage the ozone layer are undoubtedly the most important alternatives in this process. At this point, CO_2 gas emerges as an effective solution. CO_2 has been widely used in the development stages of the refrigeration industry. However, it has been replaced by halocarbon refrigerants due to the decrease in the cooling coefficient and high operating pressures that occur due to heat transfer around or above the critical point [4]. Due to the negative effects of halocarbon refrigerants on the environment, it has begun to be used again as alternative, natural refrigerant. Thanks to the current machine and heat exchanger technology and system control elements, CO_2 efficiency has reached competitive levels in the northern countries with the transcritic cycle and in the southern countries with the subcritical cascade cycle. R744 (CO_2) requires a number of additional technical requirements compared to other conventional refrigerants due to its low critical point temperature of 31.06 ° C and a high critical point pressure of 73.8 bar.

1.1.Literature Review

There are some numerical and experimental studies about CO_2 heat pumps and its applications. The literature review on this study has generally been studied on numerical analysis of CO_2 heat pumps. Some examples of this studies done are as follows.

Supriya Dharkar (Purdue University) studied at CO_2 heat pumps for commercial building applications. This study mention about a data center on the Purdue University, West Lafayette campus is used as a case study. System simulations are carried out to determine the feasibility of the system for a year using CO_2 heat pumps. Through the article it is concluded that 2-stage compression with intercooler during the summer months increases the efficiency of the system. Adding an expansion work recovery device improves the primary energy savings by 40%.[5]

Jørn Stene worked on CO_2 heat pump system for hot water heating. The scope of this thesis is limited to brine-to-water and water-to-water heat pumps connected to low-temperature hydronic space heating systems. Through the doctoral study it is concluded that the CO_2 heat pump unit covers the entire DHW (Domestic Heat Water) heating demand, and the annual heat delivered for DHW production is minimum 25 to 30% of the total annual heat delivered from the heat pump. In addition this the integrated CO_2 heat pump system will be more complex than the state-of- the art residential heat pump systems due to the requirement for a tripartite gas cooler, extra valves and tubing for by-pass of fluids, an inverter controlled pump in the DHW circuit as well as an especially designed DHW storage tank. The application of optimum high-side pressure control will further increase the technical and ope-rational complexity of the system. [6]

Arif Emre Özgür et al. worked on fluid heat pumps. In this study, the use of a two-stage transcritical CO_2 fluid heat pump system for space heating was investigated. Performance analysis has been made considering different operating conditions for the system. It is concluded that the heating efficiency coefficients of CO_2 refrigerant heat pumps can be quite high. It is seen that a competitive performance can be achieved by significantly lowering the temperature of CO_2 with the space heater and internal heat exchanger components before the two-stage compression and throttle valve.[7]

1.2.The History of R744(CO_2)

R744 (CO_2) was first introduced as refrigerant in 1850 by British Alexander Twining. However, the first CO_2 cooling system was built at the end of the 1860s by the American Thaddeus S.C.

It was carried out by Lowe. It was widely used in ships and industry until the 1920s due to its clean and reliable nature. With the introduction of CFCs in 1928, CO_2 was gradually left out of the market due to the above reasons, and its use ceased in the 1950s. By the end of the 20th century, as the restrictions on CFCs intensified, new searches were started and old, natural fluids such as CO_2 and NH3 were brought back to the agenda. In 1990, Prof. The patent application of the transcritical CO_2 cycle of Gustav Lorentzen has created a milestone for this issue [8].

1.3.Carbon Dioxide (R744-CO_2) Properties

Natural refrigerants are naturally occurring, ecologically safe working fluid. There are few different types of refrigerants in this group like Carbon-dioxide (CO_2), Ammonia (NH3) etc. Out of these natural refrigerants, from an environmental point of view carbon dioxide (R-744) regarded as a best working fluid since it is non-toxic, non-flammable and neither contributes to ozone depletion nor global warming. In 1993 Lorentzen and Pettersen rediscovered Carbon-dioxide (CO_2, R-744) as a working fluid for refrigeration and air-conditioning. Due to its environment friendliness, low price, easy availability, non-flammability, non-toxicity, compatibility with various common materials, compactness due to high operating pressures, excellent transport properties made it best working fluid.

Table 1- General Properties of Carbon Dioxide [9]

Refrigerant	R-744
Chemical formula	CO_2
Critical Temperature (°C)	31.1
Critical Pressure (kPa)	7384
Critical Density (kg/m³)	466.5
Boiling Point at Atm. Pressure (°C)	-78.4
Flammability	No
Toxicity	No

Carbon dioxide has unique properties which if integrated appropriately can be used to advantage. Carbon dioxide is colorless, odorless, and heavier than air. With a Global Warming Potential of 1, CO_2 is the reference value for comparing a refrigerant's direct impact on global warming. It is non-flammable and non-toxic making it a refrigerant with A1 safety classification

(the same as most fluorocarbon refrigerants). CO_2 as a refrigerant is sourced from a number of production methods as a by-product. Though it is nontoxic, oxygen will start getting displaced if enough carbon dioxide builds up in an enclosed space, leading to asphyxiation to anyone present over a certain period within the space. In terms of environmental impact, CO_2 does not lead to any harmful decay products.

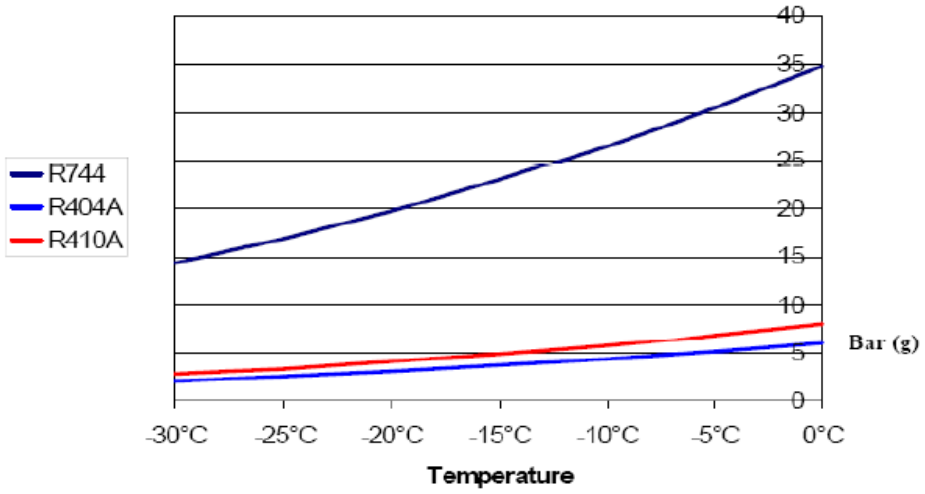

Figure 1 - Comparison of Pressures of Different Types of Refrigerants[10]

CO_2 as a refrigerant has several unique properties. The most significant being higher operating pressure of CO_2 systems. Adding to this are the extremely low viscosity and the low critical temperature of Carbon dioxide. It is now possible to source compressors for use in refrigeration system up to 16 MPa . The high pressure of CO_2 delivers many of the inherent benefits of the system. The compressors are relatively small and so is the pipework. The gas is dense and hence results in good transport and heat transfer properties. If a system is designed to capitalize on the advantage of high pressure, CO_2 systems can offer significantly more efficient systems. The viscosity of liquid CO_2 is one-tenth of water at 5°C. Unlike brine and glycol solutions, the viscosity of CO_2 at lower temperatures of -50°C remains uniform. This makes CO_2 an attractive heat transfer fluid at low temperature.

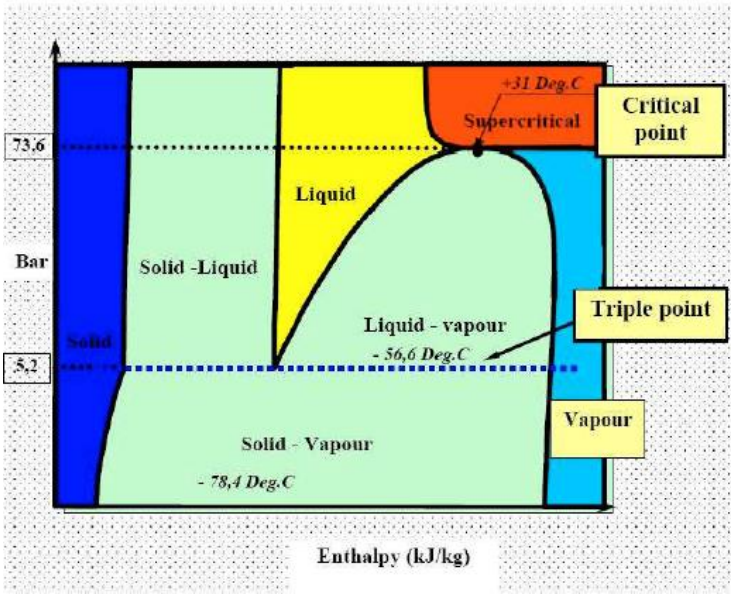

Figure 2- Pressure-Enthalpy Diagram of R744[10]

The critical temperature of CO_2 is 31°C which is considerably low compared to the other refrigerants. This offers unique opportunities to design a system in a suitable way so as to generate significant savings when compared to conventional technology. Heat recovery at these higher temperatures is very advantageous. Various water heaters, domestic, commercial and light industrial heat pump system installation in the market show that if this property is tapped in appropriately, the system can have significant advantages. The benefits of this property are more noteworthy when both, the cooling and heating systems are integrated.

Because of the above characteristics, carbon dioxide systems are best suit in Heat Pumps for heating and cooling, several researches have been carried out in these sectors proved the above statement [9].

1.4.The Comparison of CO_2 with Other Refrigerants

There are two basic concepts related to the environmental properties of refrigerants.

1. ODP (Ozone Depletion Potential): It refers to the damage that a gas can cause to the ozone layer. It is found as a relative value [11].
2. GWP (Global Warming Potential): It is the value that gives the global warming effect of a greenhouse gas to the environment relative to CO_2 in a certain period of time by assuming GWP of CO_2 is 1 [11].

The ozone depletion potential of CO_2 is zero (ODP = 0) and its direct impact on global warming is very low (GWP = 1). Table 1 gives the environmental properties of common refrigerants.

Table 2-Properties of Some Refrigerants [10]

Fluid	Boiling point (°C)	Critical temperature (°C)	Critical pressure (bar)	ODP [1]	GWP (100 yrs)	Oil	Flam.
R12	-29	100.9	40.6	0.9	8100	mineral	no
R22	-40.8	96.2	49.8	0.055	1500	mineral	no
Pure HFCs							
R23	-82.1	25.6	48.2	0	12000	ester	no
R32	-51.6	78.4	58.3	0	650	ester	**yes**
R125	-48.5	68.0	36.3	0	2500	ester	no
R143a	-47.6	73.1	37.6	0	4300	ester	**yes**
R134a	-26.5	101.1	40.7	0	1200	ester	no
R152a	-25.0	113.5	45.2	0	140	ester	**yes**
HFC mixtures							
R407C[3]	-44.0	86.8	46.0	0	1600	ester	no
R410A[2]	-50.5	72.5	49.6	0	1900	ester	no
R404A[2]	-46.4	72.1	37.4	0	3300	ester	no
Natural refrigerants							
R290 (propane)	-42.1	96.8	42.5	0	< 20	mineral	**yes**
R600a (isobutane)	-11.7	135.0	36.5	0	< 20	mineral	**yes**
CO_2 (R744)	-56.6 @ 5.2 bars	31.0	73.8	0	1	PAG	no
R717 (ammonia)	-33.3	132.2	113.5	0	0	mineral	**yes**

In addition to the concepts of ODP and GWP, the concept of Total Equivalent Warming Effect (TEWI) is also available in the literature. Total Equivalent Warming Effect (TEWI) describes the direct and indirect global warming effect of the fluid and the system on which it is located. The effect of the fluid in the environment is a direct effect due to its properties. The CO_2 emission that occurs during the energy supply to the cooling system in which it is used is an indirect effect. The sum of both effects is defined as the Total Equivalent Warming Impact (TEWI). CO_2 is also an effective fluid in reducing the total equivalent warming effect in cooling systems [12].

1.5.CO_2 Heat Pumps Usage Areas

It is possible to achieve very high effective temperatures with CO_2. For this reason, CO_2 is particularly suitable for the provision of heat in municipal and industrial heating networks, as well as in drying technology, such as in automotive paint shops. CO_2 technology is also ideally suited for all applications that require colder and warmer temperatures simultaneously – a hotel could use it, for example, for its air conditioning and even its hot water supply. The range of applications is increasing steadily; CO_2 heat pumps are now being used more and more frequently in the fields of industry and business in particular.

Building technology

- Heat supply for properties
- Cold supply for properties
- Hospitals
- Large, energy-intensive buildings (e.g. data centers, media complexes)
- Hotel complexes

Central building services engineering

- Local heat networks (e.g. belonging to public utilities and local authorities, private energy suppliers, energy service providers)
- Industrial heat and cold supply networks

Process technology

- Condensation dehumidification in process air tehcnology (painting systems, coating systems)
- Hot water creation for washing and cleaning processes (food, meat, product washes) with cold generation where necessary
- Hot air generation for drying processes (sludge, biomass, washed products) with cold generation possible
- Air preheating for spray dryers, power plants and heat generation plants

Refrigeration technology

- Cooling brine systems fort he food, pharmaceutical and chemical industries
- Commercial refrigeration
- Ice rinks [13]

In addition to these applications, the following application can be given as an example.

1.5.1.Vending machines and bottle coolers

Transcritical R744 cycles are also used for small commercial refrigeration systems. The Coca Cola Company (TCCC) has pledged to reduce to the lowest possible its uses of synthetic

refrigerants. As of year 2007, they operate 6000 transcritical vending machines with duties ranging from 300 W to a few kW.

Figures 3 and 4 show the cassette type refrigeration system working with R744.

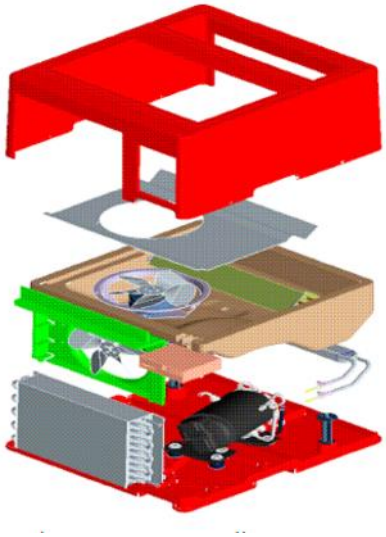

Figure 3- R744 Cycle Components[10]

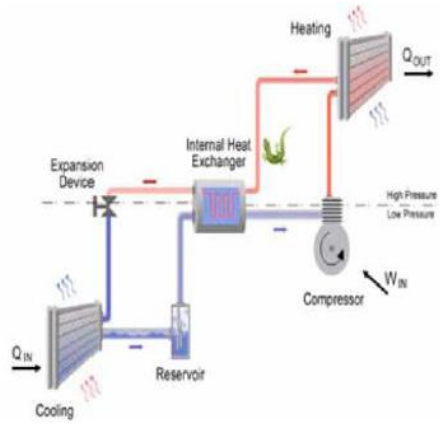

Figure 4- R744 Cooling Cassette[10]

Figure 5 shows the product range potentially covered by transcritical cycles.

Figure 5- Coca Cola Vending Machines[10]

1.6.Transcritical CO_2 Heat Pump System And Comparison With Conventional Subcritical Vapor Compression System

A transcritical CO_2 heat pump cycle is quite different from a conventional subcritical vapour compression heat pump cycle, a transcritical cycle operate beyond the critical pressure where a conventional subcritical vapour compression cycle operates under the critical pressure of the working fluid.

In a transcritical CO_2 heat pump system the heat from the source was absorbed by refrigerant in evaporator get compressed in a compressor to a desired pressure which is above the critical pressure of the refrigerant, the heat gained in the compression process is given off through the gas-cooler where the heat is given or rejected to the desired space or heating medium at an unusual large temperature glide.

Usually a condenser is used in conventional subcritical vapour compression heat pump system to give off the heat. Cooled refrigerant from the gas cooler is passed through an expansion device to bring the pressure under critical pressure and passes through the evaporator again continues the cycle.

A CO_2 heat pump system offers several unique possibilities such as simultaneous refrigeration and water heating /steam production, simpler control of capacity makes transcritical CO_2 heat pump system more suitable for air-conditioning and heat pumps due to the temperature glide at gas-cooler.

Table 3- Main Differences Between Trancritical and Subcritical R744 Heat Pump Cycle [10]

Cycle Parameters	Subcritical (CO_2)	Transcritical (CO_2)
High Pressure Cooling	Condenser-Vapor condenses at constant temperature	Gas cooler-CO_2 undergoes large temperature change
Discharge Pressure	from 10 to 40 bars	from 90 to 130 bars
Suction Pressure	from 2 to 9 bars	from 25 to 50 bars
Refrigerant Discharge Temperature	Usually less than 95 ℃	Up to 140
Expansion Device Control	By superheat set point or fixed flow expansion device	Usually used to control high pressure of CO_2
High Pressure Control	Not controlled-Pressure is set by condensation temperature-usually max 40 bars	Required -up to 130 bars
Refrigerant State	Partly liquid and partly vapor	Gas (supercritical) above 31℃ ambient ; vapor-liquid mixture below 31℃ . Can become solid upon cooling below P<6 bars.
System Pressure	Refrigerant vapor pressure at ambient air temperature	At least 74 bars -can be higher, depending on charge and temperature

1.7.Components of Transcritical R744 Heat Pumps

Components for R744 systems have to withstand much higher pressures than their HFC and HCFC counterparts. Pressure differentials are higher by one order of magnitude. Other issues are introduced by the particularity of R744, e.g. high discharge temperatures, compatibility with lubricating oils, potential degradation of seals after decompression, etc. These issues hinder the fast development of a "component chain".

1.7.1.Compressors

Air compressor is a machine that is capable of converting electric power into kinematic energy specifically by utilizing compressed air. When the air is released in quick burst it releases an amount of kinetic energy that can be harnessed for a number of purposes including pneumatic device activation, air transfer and cleaning operations.

Figure 6- A simple standard air compressor [14]

There are some advantages and disadvantages of R744 compressors. It has low compression and high volumetric efficiency and low sweeping volume. In applications at very low temperatures, the discharge line temperature increases too much. Significant reinforcement is required in the outer shell and other components due to high operating pressures. [10]

1.7.2.Throttling Valves

Throttling valves are any kind of flow-restricting devices that cause a significant pressure drop in the fluid. Unlike turbines, they produce a pressure drop without involving any work. The pressure drop in the fluid is often accompanied by a large drop in temperature, and for that reason throttling devices are commonly used in refrigeration and air-conditioning applications.

Figure 7-A simple throttling valve[15]

Table 4- Comparison of Expansion Valves [10]

	Capillary Tube / Orifice	**Mechanical Expansion Valve**	**Thermostatic Expansion Valve**	**Electronic Expansion Valve**
Advantages	Simple and cheap	It reacts according to variable capacity.	It corresponds according to the variable temperature outside.	It provides full control and optimization to the system.
Disadvantages	It works optimally only under specified conditions.	It has only one set value, it does not react sufficiently to the variable temperature in the outdoor environment.	It does not optimize according to variable capacity.	They are expensive and complex systems.

1.7.3.Evaporators

Another name of the vaporizer used in refrigeration systems is evaporator. Vaporizer is also called cooling coil. Evaporator in refrigeration system is; entrance of coolant as fluid and outgoing as gas after evaporation. When the coolant fluid enter into the channels of evaporator soak up the heat from the refrigerated element or ambient and at the time soaking up it starts to boil and vaporize. At the end of these processes, evaporator realizes the general goal of all system.

Figure 8 – A Standard Evaporator [15]

1.7.4.Gas Cooler

The gas cooler is a multi-pass cross-counterflow, water-coupled heat exchanger intended for heating water. The heat exchanger is composed of several finned plates that function as water passes and multiple microchannel refrigerant tubes.

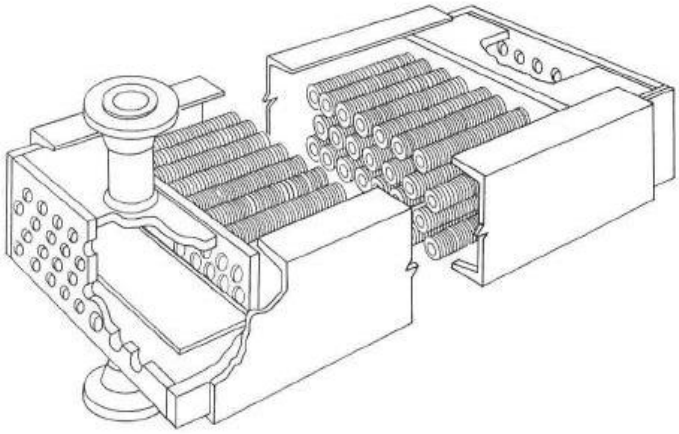

Figure 9- A Standard Gas Cooler [14]

1.7.5.Internal Heat Exchangers(IHX)

Heat exchangers are devices that facilitate the *exchange of heat* between *two fluids* that are at different temperatures while keeping them from mixing with each other. Heat exchangers are commonly used in practice in a wide range of applications, from heating and air-conditioning systems in a household, to chemical processing and power production in large plants. Heat exchangers differ from mixing chambers in that they do not allow the two fluids involved to mix. In a car radiator, for example, heat is transferred from the hot water flowing through the radiator tubes to the air flowing through the closely spaced thin plates outside attached to the tubes.[16]

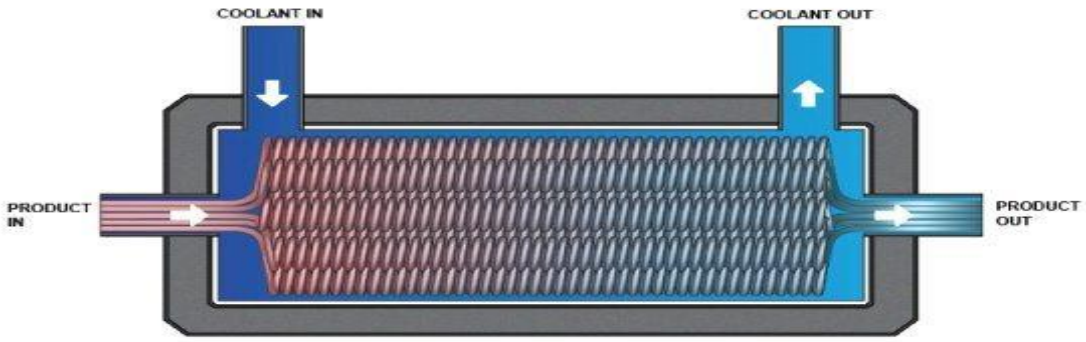

Figure 10- A Standard Internal Heat Exchanger

1.7.6.Flash Tank

A flash tank serves as a collection system for a variety of condensate drain lines. Flash tanks receive high pressure condensate which is then exposed to a low pressure steam source. When this occurs, a certain percentage of condensate will “flash” to steam at the lower pressure. This

steam can be "recycled" on other low pressure steam heat transfer devices. Smaller in size than traditional flash tanks, flash separators utilize cyclonic action to instantly separate steam and condensate.

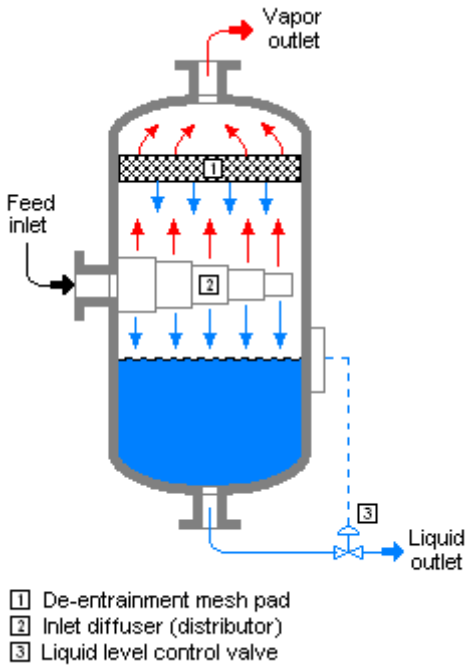

Figure 11-The schematic diagram of the Flash Tank

1.8. Alternative Systems of CO_2 Heat Pumps

1.8.1. Heating Demand in Residential Buildings

The heating demands in a residential building are caused by transmission and infiltration losses through the building envelope, ventilation losses when fresh air is supplied to the building by means of a ventilation system, and heating of domestic hot water (DHW). The transmission and infiltration losses in new buildings have been considerably reduced in recent years. Various standards for low-energy houses have also been established in Europe, the USA and Canada. The annual transmission and ventilation losses in these houses are typically 40 to 50% lower than that of new residential buildings which are designed in accordance with prevailing building regulations (Breembroek and Dieleman, 2001).

Owing to the decreasing space heating demand and the fact that about 70% of the ventilation losses in balanced ventilation systems can be recovered by heat exchange, the annual heating demand for DHW constitutes an increasing share of the total heating demand in new buildings.

Figure 12 shows, as an example, the development of the different heating demands in single-family houses (Breembroek and Dieleman, 2001).

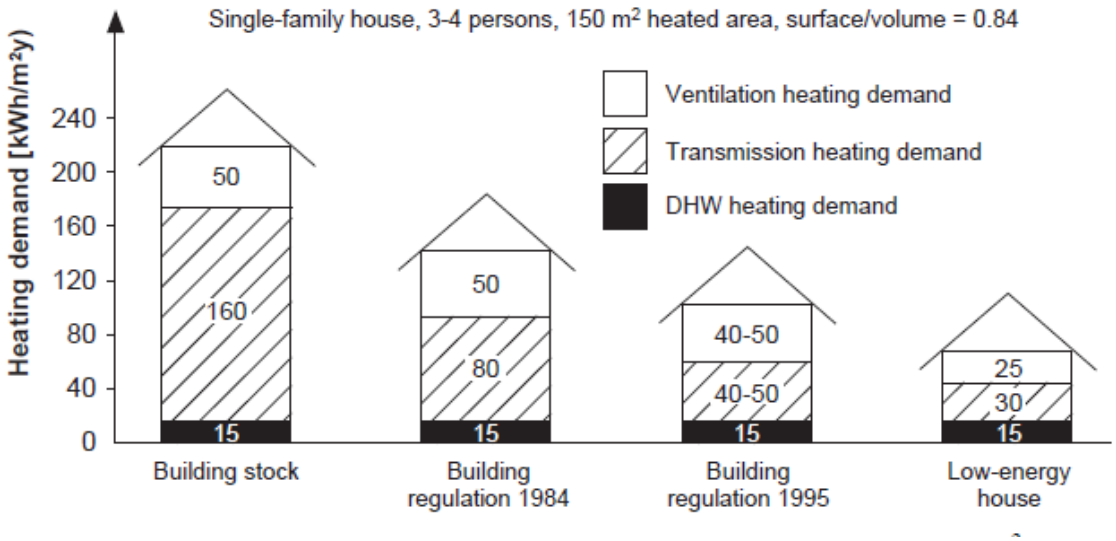

Figure 12- The Different Heating Demands In Single-Family Houses [9]

1.8.2. Residential Basic Transcritical CO_2 Heat Pumps Systems(BTS)

Owing to the favourable environmental and thermophysical properties of carbon dioxide (CO_2), many universities, research institutions and companies have in recent years been analysing and testing various types of residential CO_2 heat pump systems. Some applications include CO_2 heat pump water heaters, CO_2 heat pumps in combination with low-temperature heat distribution system, Integrated CO_2 heat pump systems for space heating and hot water heating in low-energy houses and passive houses etc.

Lorentzen (1994) reintroduced CO_2 as a working fluid, and demonstrated that the production of DHW is one of the most promising applications for the transcritical CO_2 heat pump process. The high energy efficiency of the CO_2 heat pump water heater is due to the good temperature fit between the CO_2 and the water in the counter-flow gas cooler, the excellent heat transfer properties of CO_2 and the high compressor efficiency. Another advantage of the CO_2 heat pump water heater is the capability of supplying high-temperature DHW, which eliminates the requirement for supplementary heating.

In recent years, a number of prototype CO_2 heat pump water heaters have been tested. Virtually all installations have been single-stage units using a low-pressure liquid receiver (LPR), a suction gas heat exchanger and a counter-flow tube-in-tube gas cooler. The principle of the CO_2 heat pump water heater is presented in Figure 13.

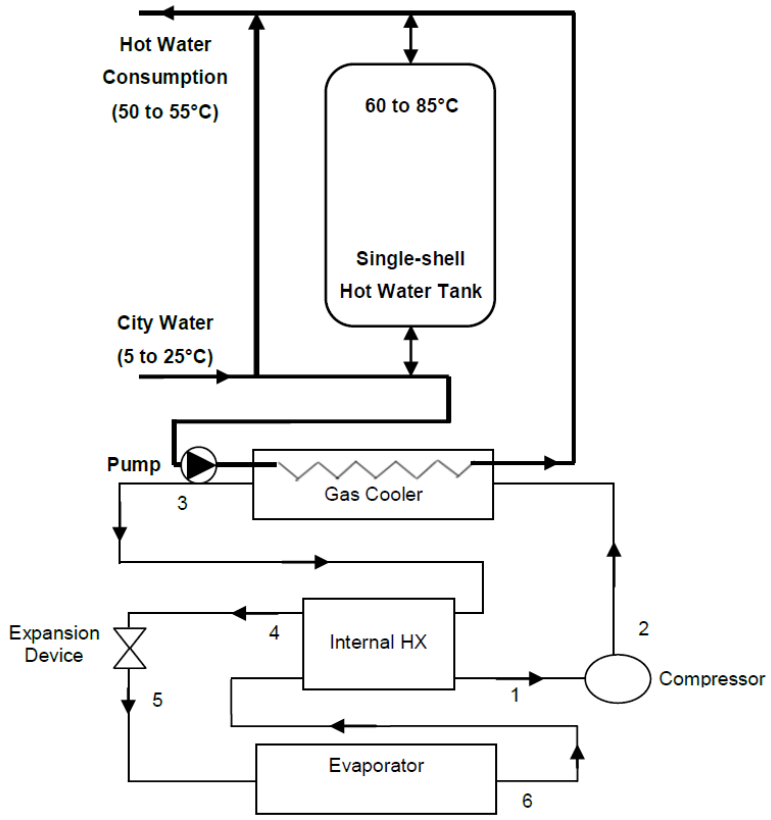

Figure 13-Basic CO_2 Heat Pump Water Heater [9]

1.8.3. Basic Two-Stage Cycle (BTC) with Two Compressors

As well known, there are various types of two-stage transcritical CO_2 cycles for refrigeration and heat pump applications. In this study, we select the two-stage cycle with a flash tank and an internal heat exchanger as baseline cycle. Figure 14 shows the schematic system for the basic two-stage cycle (BTC), respectively. The cycle components for the BTC cycle include a high-pressure (HP) compressor, a low-pressure (LP) compressor, a condenser, an internal heat exchanger (IHX), a flash tank, two expansion valves (TEVs) and an evaporator.

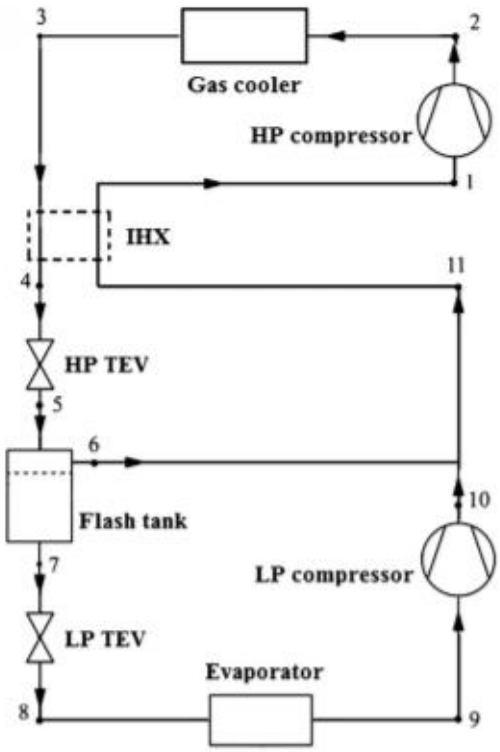

Figure 14-The BTC cycle schematic system

In addition, some assumptions are made to simplify the analysis:

(1) All components are assumed to be a steady-state and steady-flow process.

(2) The throttling process in the expansion valve is isenthalpic.

(3) Refrigerant pressure and heat losses in the cycles are neglected.

1.8.4.An Ejector Enhanced Sub-Cooler Vapor Injection CO_2 Heat Pump Cycle (ESCVI)

Layout diagram of the ESCVI cycle is depicted in Figure 15. ESCVI system consists of a CO_2 vapor-injection compressor (such as twin rotary compressor), a gas cooler, an evaporator, an ejector, a separator and two expansion valves. The cycle actual working principle is described as follows: the superheated gas discharged by compressor (state 4) enters into the gas cooler where it rejects the heat to the secondary flow (water) and becomes low temperature and high-pressure gas (state 5), and the supplied water is once heated to the desired temperature in the gas cooler by countercurrent heat exchanging with CO_2 (process 17-18) and then is filled into a storage tank.

Then the high-pressure refrigerant leaving the gas cooler is split into two streams. The principal branch enters into the sub-cooler to obtain further cooled by the other branch with intermediate temperature produced by throttling process in the EP2. The sub-cooled refrigerant (state 8)

enters the nozzle of the ejector as the primary flow and entrains the vapor from the evaporator (state 14), and then the two-phase mixed flow (state 11) leaves the ejector with a pressure rise after mixing and diffuser sections.

The two-phase flow entering into the separator is separated into saturated vapor and liquid flow. The saturated liquid (state 12) enters the evaporator to absorb the heat from the surroundings after a pressure reduction through EP2. The saturated vapor (state 1) enters the compressor and obtains the first-stage compression in the low-pressure cylinder, and then the low-pressure discharged vapor at an intermediate pressure mixes with the saturated vapor from sub-cooler. The mixed flow (state 3) enters into the second-stage compression cylinder and then is discharged with high temperature and pressure (state 4). In this way, a complete ESCVI cycle is completed.

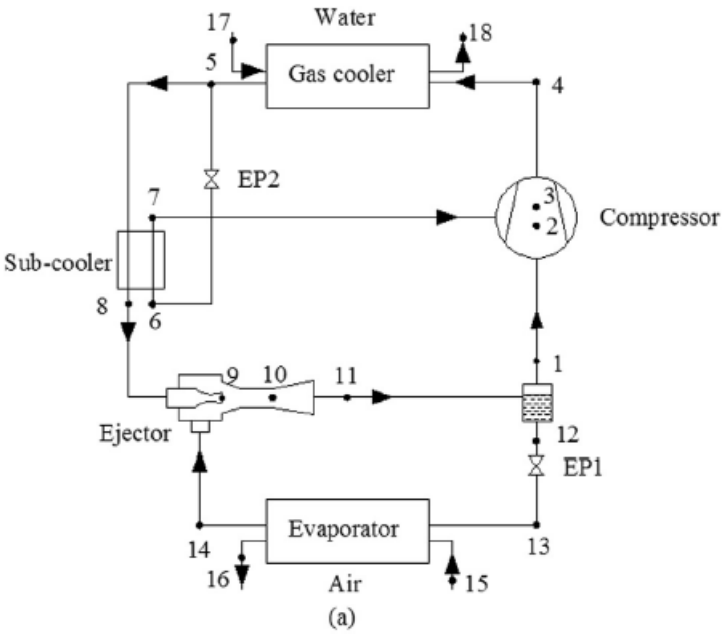

Figure 15-The Schematic System of ESCVI Cycle

1.8.5. Two-Stage Transcritical CO_2 Heat Pump Cycle with Double Ejectors (ETC)

Two two-phase ejectors and an additional flash tank are introduced as a new modification to improve the cycle performance. Figure 16 shows the schematic system for the ejector-expansion two-stage cycle (ETC). The working principle of the ETC cycle is described as follows: the compressed refrigerant vapor coming from HP compressor (point 2) is passed from the gas cooler through the IHX to the HP ejector (points 3 and 4), where the high pressure refrigerant further entrains the refrigerant vapor from LP compressor (point 13); the two-phase mixed fluid from the HP ejector (point 5) is then separated into the vapor and the liquid by the

HP flash tank (points 6 and 7); the vapor refrigerant returns to the HP compressor, and the liquid refrigerant enters the LP ejector and further entrains the refrigerant vapor from the evaporator (point 11); the two-phase mixed fluid from the LP ejector (point 8) is separated into the vapor and the liquid by the LP flash tank (points 9 and 12); the vapor is compressed by the LP compressor, and the liquid is transferred through the expansion valve to the evaporator (point 10) where it is vaporized completely. Note that points 4', 5', 7' and 8' represent the refrigerant states in the two ejectors, and the working process of each ejector is omitted for simplicity.

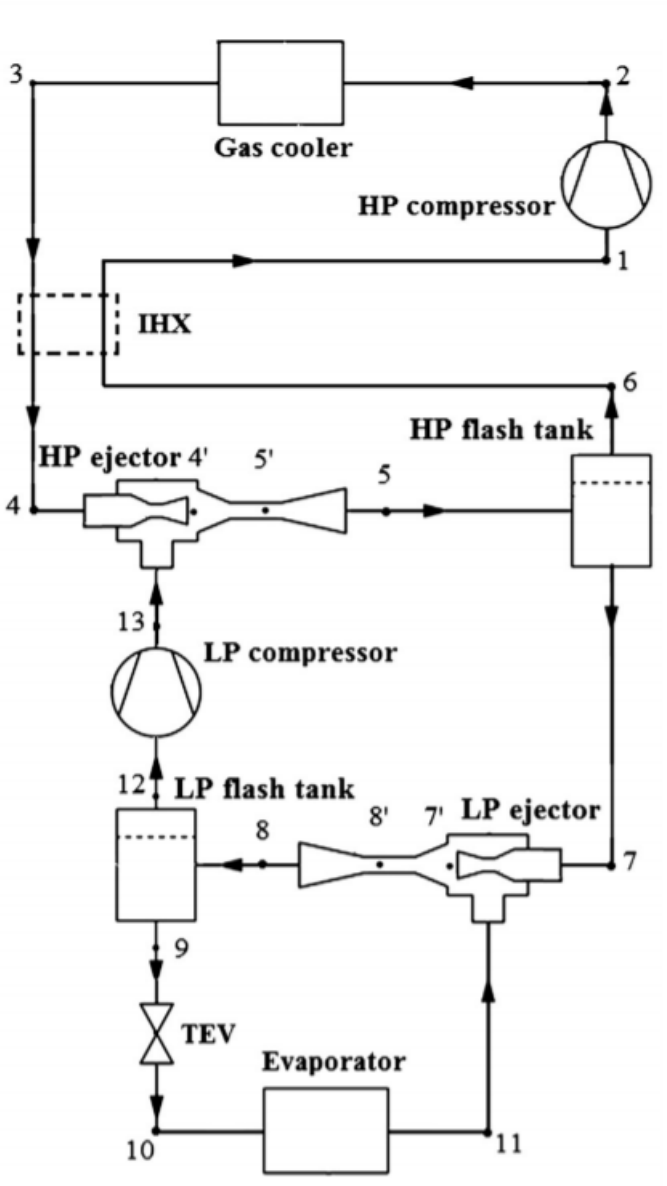

Figure 16-The Schematic System of ETC Cycle

2.METHODOLOGY

2.1.Thermodynamic Analysis of CO_2 Heat Pumps Components

To simulate a residential CO_2 heat pump system for space heating and domestic hot water, a heat pump cycle model was developed based on energy balance of individual components of the cycle.

The cycle consists of a compressor, gas-cooler, internal heat exchanger, evaporator and an expansion device. Following are general assumptions have been made in this simulation,

1. Only the steady state solution is being analyzed.

2. Heat losses from the heat exchangers and expansion device are neglected.

3. Pressure drop in Heat exchangers, connection pipelines, bends and water side are assumed negligible.

4. Changes in kinetic and potential energies are negligible.

5. UA values (overall heat transfer coefficient, U, multiplied by the heat transfer area, A) of heat exchanger were taken as examples of different systems.

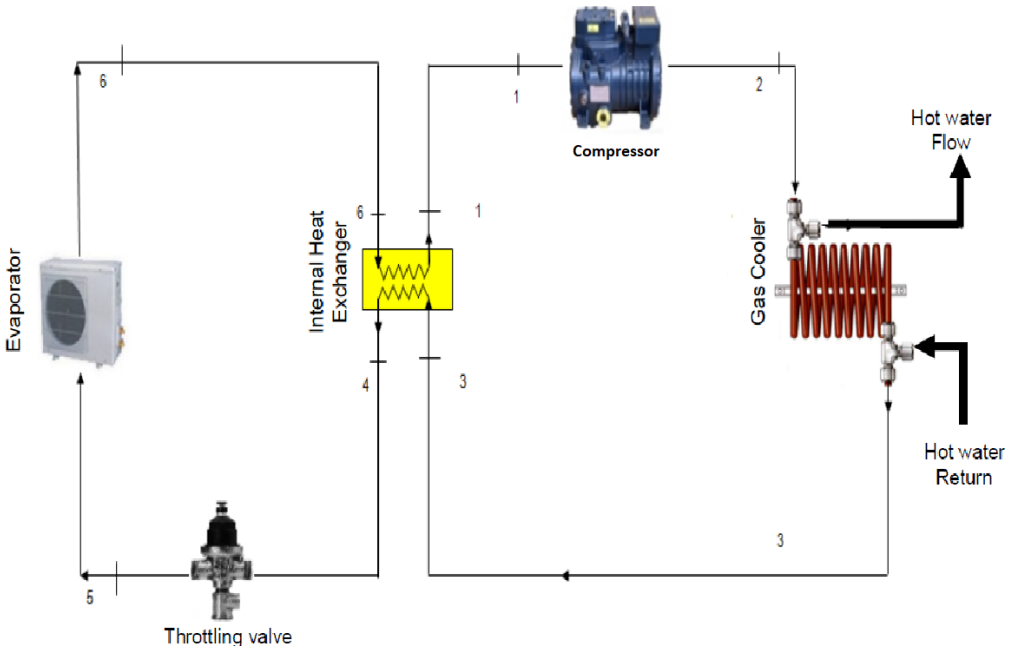

Figure 17- Transcritical CO_2 Heat Pump with Internal Heat Exchanger [9]

2.1.1.Compressor

The steady flow energy equation for a compressor gives [15]

$$h_1 + W_{in} - h_2 - Q_{out} = 0 \quad (since\ \Delta ke = \Delta pe \cong 0) \tag{1}$$

In the folllowing statement, we were given the isentropic effiency of R744 compressors as below.[12]

$$\varphi_{compressor} = \frac{h_{2s} - h_1}{h_2 - h_1} \tag{2}$$

The exergy loss of compressor component is given by [18]

$$\dot{X}_{lost} = \dot{W}_{com} - \dot{m}_{com}[h_2 - h_1 - T_0(s_2 - s_1)] \tag{3}$$

where $\dot{W}_{com} = \dot{m}_{com}(h_2 - h_1)$ and T_0 is the environmental state temperature.

2.1.2Throttling Valves

Throttling valves are usually small devices, and the flow through them may be assumed to be adiabatic (q = 0) since there is neither sufficient time nor large enough area for any effective heat transfer to take place. Also, there is no work done (w =0), and the change in potential energy, if any, is very small ($\Delta pe = 0$). Even though the exit velocity is often considerably higher than the inlet velocity, in many cases, the increase in kinetic energy is insignificant ($\Delta ke = 0$). Then the conservation of energy equation for this single-stream steady-flow device reduces to [15]

$$h_2 \cong h_1 \ \ (kj/kg) \tag{4}$$

The exergy loss of throttling valve component is given by [18]

$$\dot{X}_{lost} = \dot{m}_{\text{throttling}\,valve}[h_1 - h_2 - T_0(s_1 - s_2)] \tag{5}$$

where T_0 is the environmental state temperature.

2.1.3.Evaporator

In this study, we assumed the evaporator exit as saturared vapor. So, temperature of refrigerant leaving evaporator has exact temperature of the outside air.[15]

The exergy loss of evaporator component is given by [18,19]

$$\dot{X}_{lost} = \left(1 - \frac{T_0}{T_F}\right) Q_{eva} + \dot{m}_{eva}[h_1 - h_2 - T_0(s_1 - s_2)] \quad (6)$$

where $Q_{eva} = \dot{m}_{eva}(h_1 - h_2)$, T_0 is the environmental state temperature and T_F is the refrigeration room temperature.

2.1.4.Gas Cooler

When the gas cooler is analysing, the effectiveness- NTU methos can use to do thermodynamic analyses.[17]

$$C_r = \frac{C_{min}}{C_{max}} \quad (7)$$

$$NTU = \frac{UA}{C_{min}} \quad (8)$$

$$\varepsilon = 1 - exp\left\{\frac{1}{C_r}.NTU^{0.22}[\exp(-C_r.NTU^{0.78}) - 1]\right\} \quad (9)$$

The exergy loss of gas cooler component is given by [19]

$$\dot{X}_{lost} = \left(1 - \frac{T_0}{T_G}\right) Q_{gc} + \dot{m}_{gc}[h_2 - h_1 - T_0(s_2 - s_1)] \quad (10)$$

where $Q_{gc} = \dot{m}_{gc}(h_2 - h_1)$, T_0 is the environmental state temperature and T_G is the gas cooler outlet temperature.

2.1.5.Internal Heat Exchanger

When the internal heat exchanger is analysing, the effectiveness- NTU methods can be used to perform thermodynamic analyses. This method is based on a dimensionless parameter called the heat transfer effectiveness ε, defined as

$$\varepsilon = \frac{\dot{Q}}{Q_{max}} = \frac{actual\ heat\ transfer\ rate}{maxiumum\ possible\ heat\ transfer\ rate} \quad (11)$$

The actual heat transfer rate in a heat exchanger can be determined from an energy balance on the hot or cold fluids and can be expressed as

$$\dot{Q} = C_c\left(T_{c,out} - T_{c,in}\right) = C_h(T_{h,in} - T_{h,out}) \quad (12)$$

where $C_c = \dot{m}_c C_{pc}$ and $C_h = \dot{m}_c C_{ph}$ are the heat capacity rates of the cold and the hot fluids, respectively.

The maximum possible heat transfer rate in a gas cooler is

$$Q_{max} = C_{min}\left(T_{h,in} - T_{c,in}\right) \quad (13)$$

where C_{min} is the smaller of $C_c = \dot{m}_c C_{pc}$ and $C_h = \dot{m}_c C_{ph}$.

The determination of $\dot{Q}_{max}$ requires the availability of the inlet temperature of the hot and cold fluids and their mass flow rates, which are usually specified. Then, once the effectiveness of the heat exchanger is known, the actual heat transfer rate $\dot{Q}$ can be determined from[16]

$$\dot{Q} = \varepsilon . Q_{max} = \varepsilon . C_{min}\left(T_{h,in} - T_{c,in}\right) \tag{14}$$

The exergy loss of internal heat exchanger component is given by [19]

$$\dot{X}_{lost} = \dot{m}_{ihe}[(h_3 - h_4) - (h_1 - h_6)] - T_0[(s_3 - s_4) - (s_1 - s_6)] \tag{15}$$

where T_0 is the environmental state temperature.

2.1.6.Flash Tank

The steady flow energy equation for a flash tank gives [15]

$$m_3 h_3 = m_1 h_1 + m_2 h_2 \quad \text{where} \quad m_3 = m_1 + m_2 \tag{16}$$

The exergy loss of flash tank component is given by [19]

$$\dot{X}_{lost} = (\dot{m}_3 h_3 - \dot{m}_1 h_1 - \dot{m}_2 h_2) - T_0(\dot{m}_3 s_3 - \dot{m}_1 s_1 - \dot{m}_2 s_2) \tag{17}$$

The state 3 represents the input of flash tank and it is mixture. The state 2 and 3 represent the outputs of flash tank. The state 2 is steam (its quality is 1), the state 3 is liquid (its quality is 0).

2.1.7.Ejector

Generally, the performance of the ejector could be assessed by entrainment ratio μ and pressure lift ratio r_p. The entrainment ratio is defined as the mass flow rate ratio of secondary to primary fluid, given as,

$$\mu = \frac{\dot{m}_{14}}{\dot{m}_9} \tag{18}$$

where $\dot{m}_{14}$ and $\dot{m}_9$ represents the mass flow rates of the secondary and primary flow of the ejector, respectively.

On the other hand, the pressure lift ratio r_p is another assessment criterion for the ejector performance, which is defined as the ratio of the ejector exit pressure P_{11} to the inlet pressure of the secondary flow P_{14}, given as,

$$r_p = \frac{P_{11}}{P_{14}} \tag{19}$$

Based on the assumptions mentioned above and the conservations of mass, momentum and energy, the detailed computational equations are expressed as follows:

Applying the energy conservation principle and neglecting the inlet velocity, the energy balance at the nozzle can be expressed as,

$$h_8 = h_9 + \frac{1}{2} u_9^2 \tag{20}$$

where h_8 and h_9 represent the specific enthalpies of the primary flow entering and leaving the nozzle, respectively.

The isentropic efficiency of the nozzle φ_n is defined as,

$$\varphi_n = \frac{h_8 - h_9}{h_8 - h_{9s}} \tag{21}$$

where h_{9s} represents the ideal exiting specific enthalpy through an isentropic expansion process in the nozzle.

In the mixing section, when the energy dissipation in the mixing process is neglected, the momentum conservation equation and the ideal mixing velocity can be expressed as,

$$\dot{m}_9 u_9 + \dot{m}_{14} u_{14} = (\dot{m}_9 + \dot{m}_{14}) u'_{10} \tag{22}$$

$$u'_{10} = \frac{1}{1+\mu} u_9 + \frac{\mu}{1+\mu} u_{14} \tag{23}$$

where the secondary flow velocity u_{14} is negligible compared with the primary flow velocity u_9, so the ideal mixing velocity can be derived as,

$$u'_{10} = \frac{1}{1+\mu} u_9 \tag{24}$$

In this paper, the energy dissipation at the mixing process in mixing chamber is taken into consideration, and the mixing efficiency φ_m is introduced to calculate the mixing velocity.

$$\varphi_m = \frac{u_{10}^2}{u'^2_{10}} \tag{25}$$

$$u_{10} = \frac{1}{1+\mu} u_9 \sqrt{\varphi_m} \tag{26}$$

Applying the energy conversation at the diffuser section of the ejector, the specific enthalpy of the mixed flow leaving the diffuser can be expressed as,

$$h_{11} = h_{10} + \frac{1}{2} u_{10}^2 \tag{27}$$

where h_{10} and h_{11} represent the specific enthalpy of the mixed flow entering and leaving the diffuser, respectively.

The isentropic efficiency of the diffuser φ_d is defined as,

$$\varphi_d = \frac{h_{11s} - h_{10}}{h_{11} - h_{10}} \tag{28}$$

where h_{11s} represents the ideal specific enthalpy of the mixed fluid at the outlet of the diffuser through an isentropic compression process.

Due to the mass conservation constraint for steady-state operation of the cycle, the quality of the mixed flow exiting the ejector x and the entrainment ratio μ should satisfy the relationship as follow,

$$x = \frac{1}{1+\mu} \tag{29}$$

When the inlet state parameters of the primary flow and the secondary flow are given and the initial entrainment ratio μ is specified, the state parameters of exit flow and the real entrainment ratio μ could be obtained by applying Eqs. (1) - (12) with an efficient iterative procedure.

3.RESULTS

3.1.Input Data and Assumptions For CO_2 Heat Pump With Internal Heat Exchanger

Water inlet, outlet temperatures and its mass flow rate are the inputs for the simulation. The flow chart shown below illustrates the simulation process in step wise manner. In the simulation, by giving the constant input parameters values like UA for heat exchangers taken from manufacturer data.

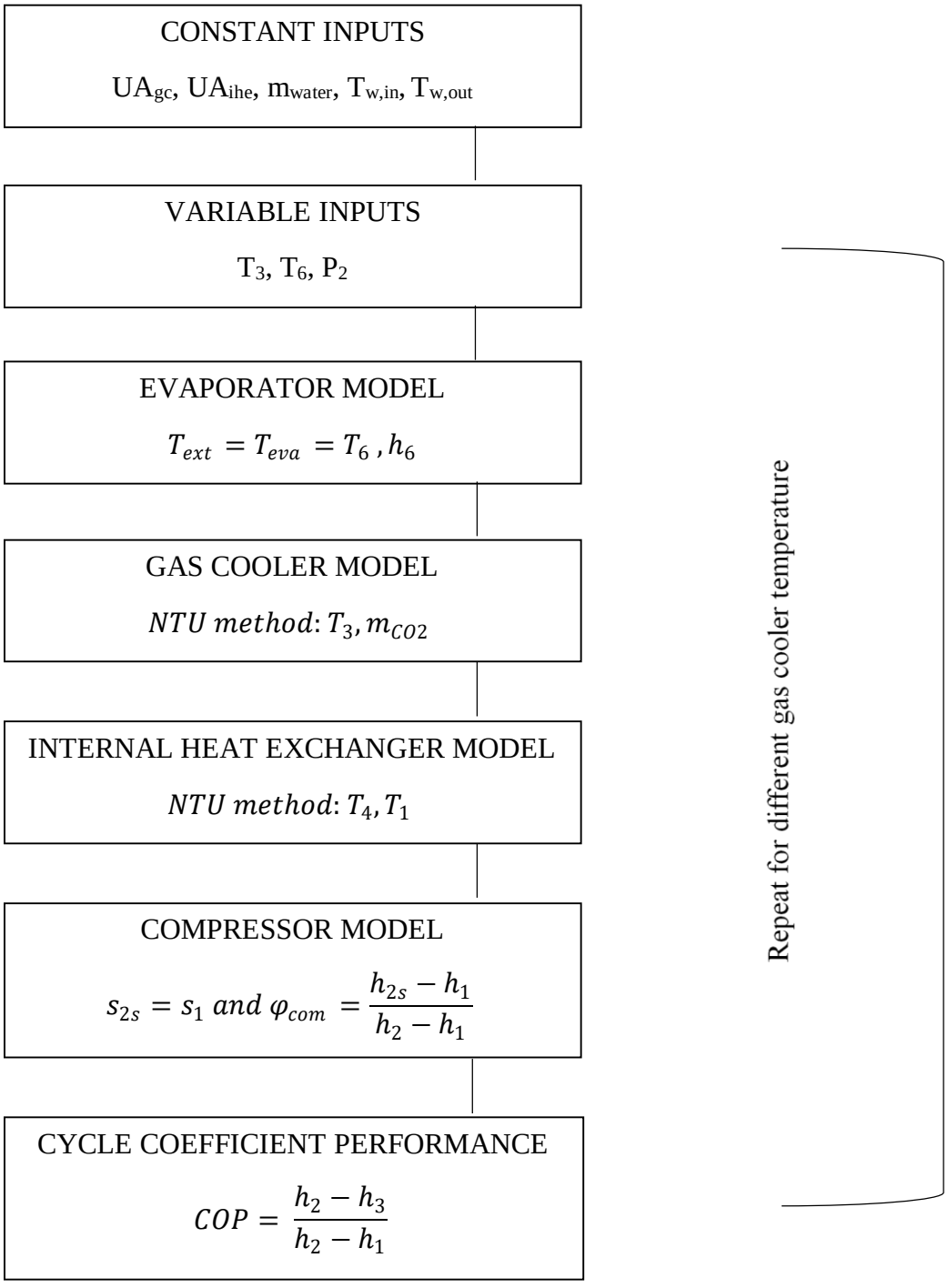

Figure 18-Flow Chart for The Numerical Solution of CO_2 Heat Pump With Heat Exchanger

Gas cooler temperature are variable inputs to examine the performance analysis of the pump. Refrigeration conditions at evaporator inlet and at gas cooler outlet as well as internal heat exchanger were calculated based on mathematical model of gas-cooler and internal heat exchanger, finally COP (Coefficient of Performance) can be calculated.

3.2.Results of CO_2 Heat Pump With Internal Heat Exchanger

The CO_2 heat pump with internal heat exchanger has been made its thermodynamic analysis using the assumptions mentioned in the previous section with EES [20] (Engineering Equation Solver).

The CO_2 heat pumps with internal heat exchanger is influenced by many parameters of the cycle. There are some important properties to achieve a high COP for the CO_2 heat pump. The gas cooler temperature depends on the following parameters;

- The inlet and outlet temperatures of water
- The pressure of compressor outlet, so high side pressure
- The characteristics of gas cooler
- The evaporator temperature
- The mass flow rate of refrigerant and water sides

Figure 19 and 20 shows T-s and P-h diagrams for a CO_2 heat pump with internal heat exchanger cycle.

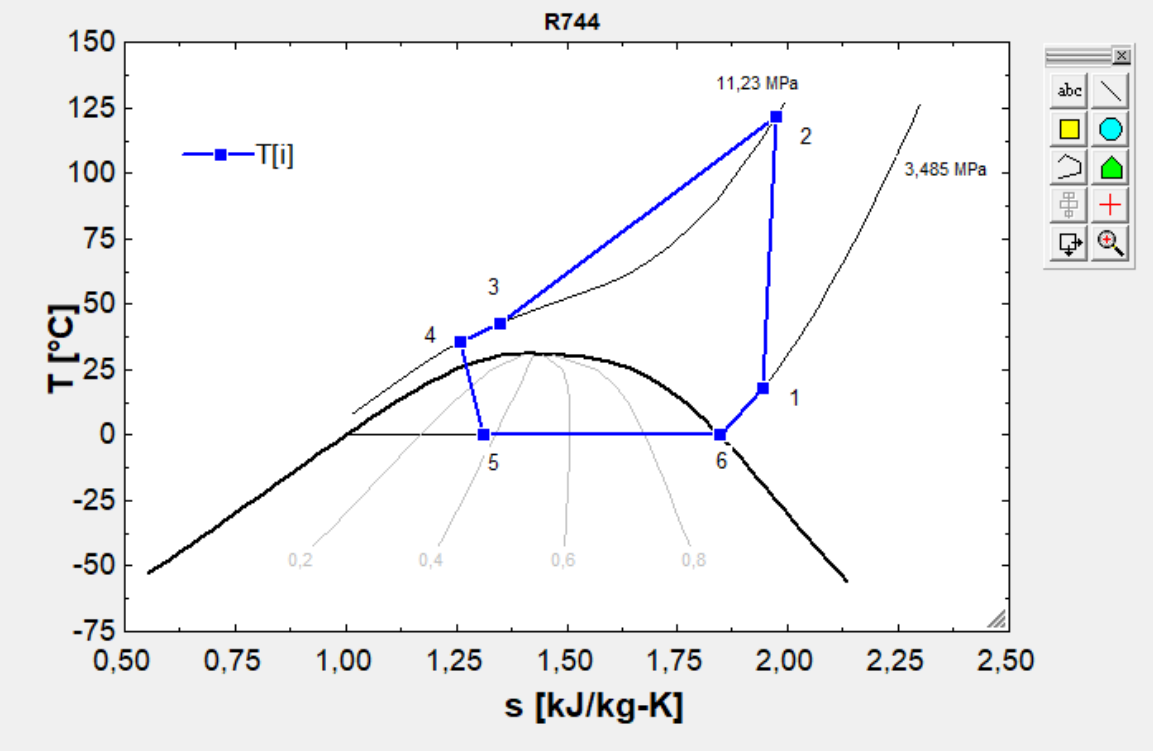

Figure 19- T-s diagram for CO_2 heat pump with internal heat exchanger cycle

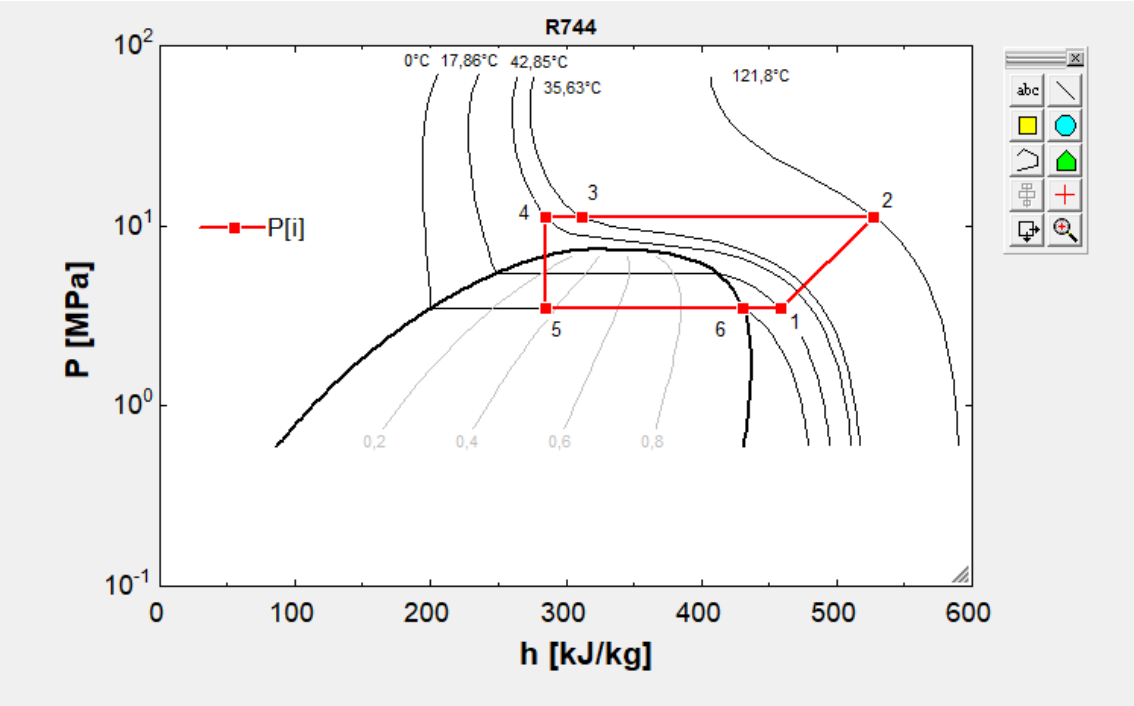

Figure 20- P-h diagram for CO_2 heat pump with internal heat exchanger cycle

The mass flow rates of water and carbondioxide fluids are kept constant to be $0.2\ kg/s$ and $0.3094\ kg/s$ respectively. The water has $20℃$ of temperature in gas cooler inlet, and the outlet temperature of water determines the high-side pressure of pump. According to the outlet temperature of water, the value that high-side pressure should take is shown in Table 5.

Table 5- The High-Side Pressure With Outlet Temperature of Water

$T_{w,out}$ (°C)	$P_2\ (MPa)$
70	9.8
75	10.5
80	11.2
85	12
90	12.8
95	13.7
100	14.7

The simulation was carried to examine the effects of gas cooler outlet temperature on COP in the cycle. The coefficient of performance was calculated for gas cooler outlet temperature at constant evaporator temperature 0℃. The gas cooler is used to heat water from 20℃ to 80℃ at a rate of $0.2\ kg/s$. The heating was to be accomplished by carbondioxide at a mass flow rate of $0.3094\ kg/s$. The gas cooler outlet temperature from 10℃ to 70℃ was taken in this analysis as shown in Figure 21. The COP decreased linearly from 10℃ to 40℃ of gas cooler outlet temperature, then the COP decreased exponentially from 40℃ to 70℃ of gas cooler outlet temperature.

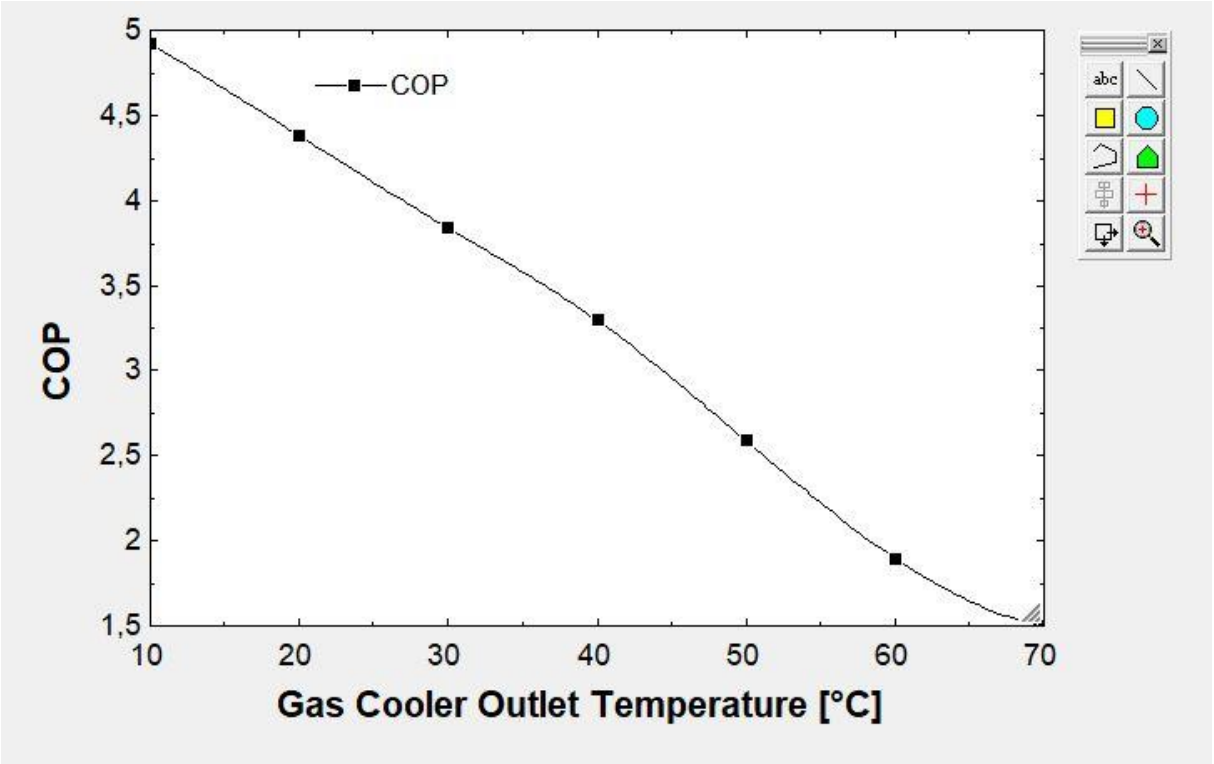

Figure 21- Graph for COP-Gas Cooler Outlet Temperature

The simulation was carried to examine the effects of evaporator temperature on COP in the cycle. The COP increased from -25 to 15 ℃ of evaporator temperature.

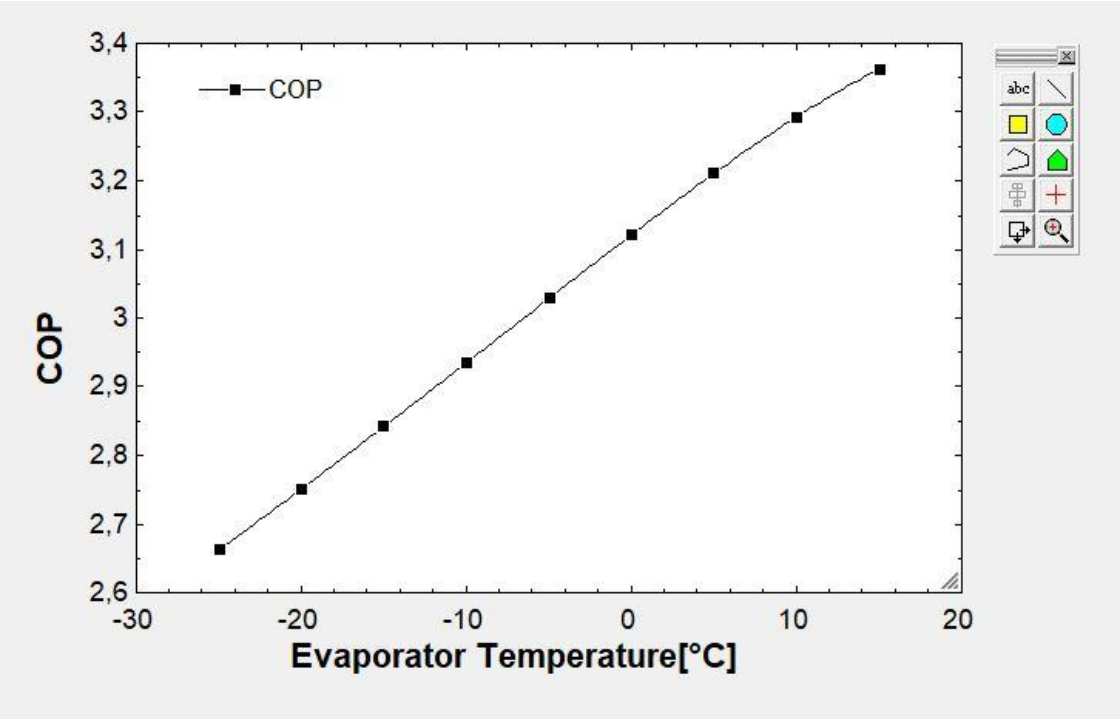

Figure 22- Graph for COP-Evaporator Temperature

The exergy analysis has been done for different evaporator temperature in EES. The maximum exergy loss was observed in the gas cooler, and the minumum exergy loss observed in the internal heat exchanger.

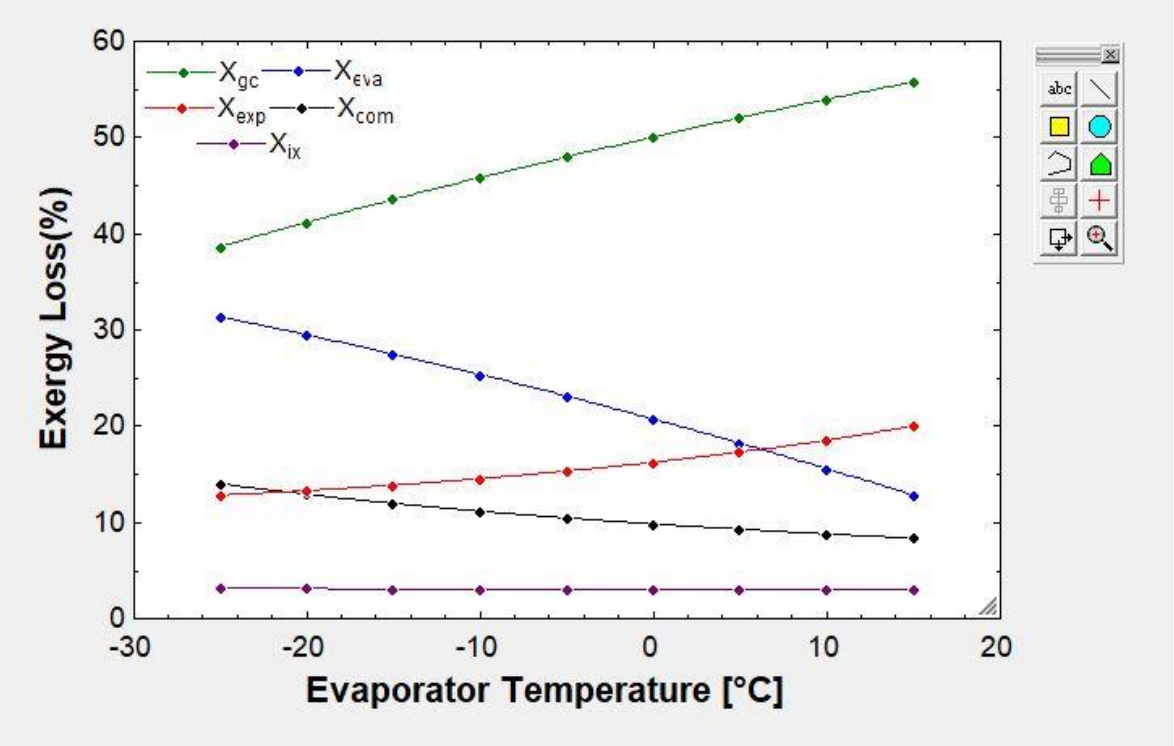

Figure 23- Component Based Exergy Lost Variation With Evaparator Temperature

3.3.Results of CO_2 Heat Pump on BTC Cycle with Two Compressors

The CO_2 heat pump on BTC cycle with two compressor has been made its thermodynamic analysis using the assumptions mentioned in the previous section with Matlab CoolProp software.

The CO_2 heat pump on BTC cycle with two compressor is influenced by many parameters of the cycle. There are some important properties to achieve a high COP for the CO_2 heat pump. The gas cooler temperature depends on the following parameters;

- The pressure of compressor outlet, so high side pressure
- The characteristics of gas cooler
- The evaporator temperature
- The degree of sub-cooling

Figure 24 and 25 shows T-s and P-h diagrams for BTC cycle with two compressor.

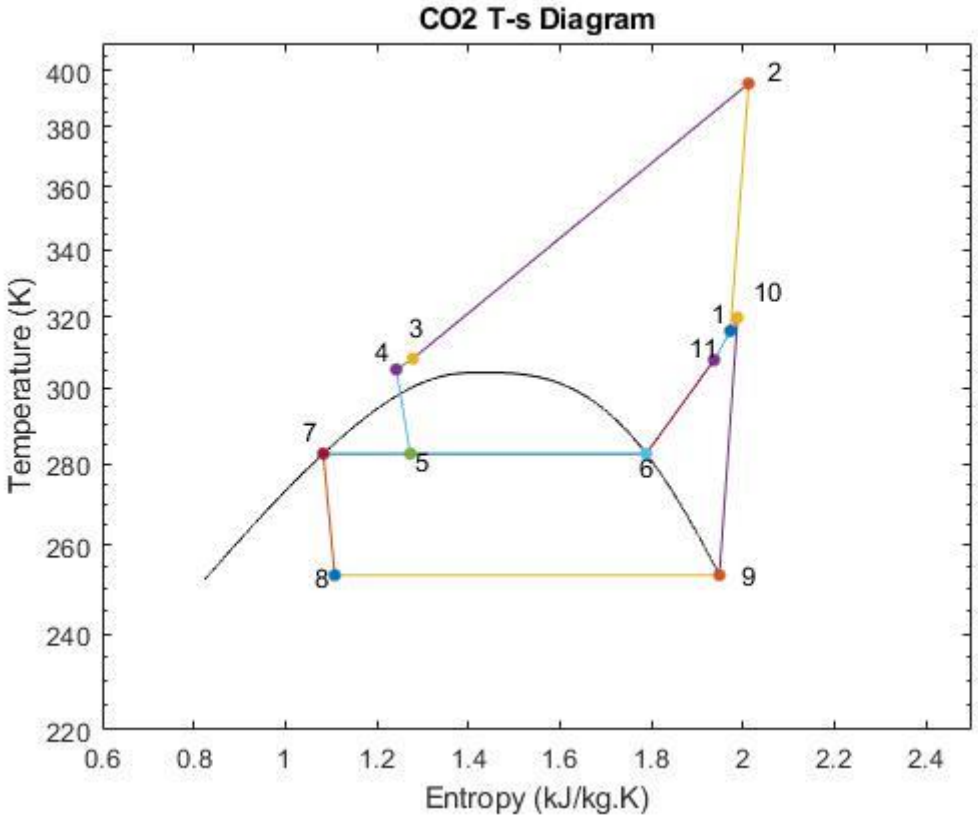

Figure 24-T-s diagram for CO_2 heat pump on BTC cycle with two compressors

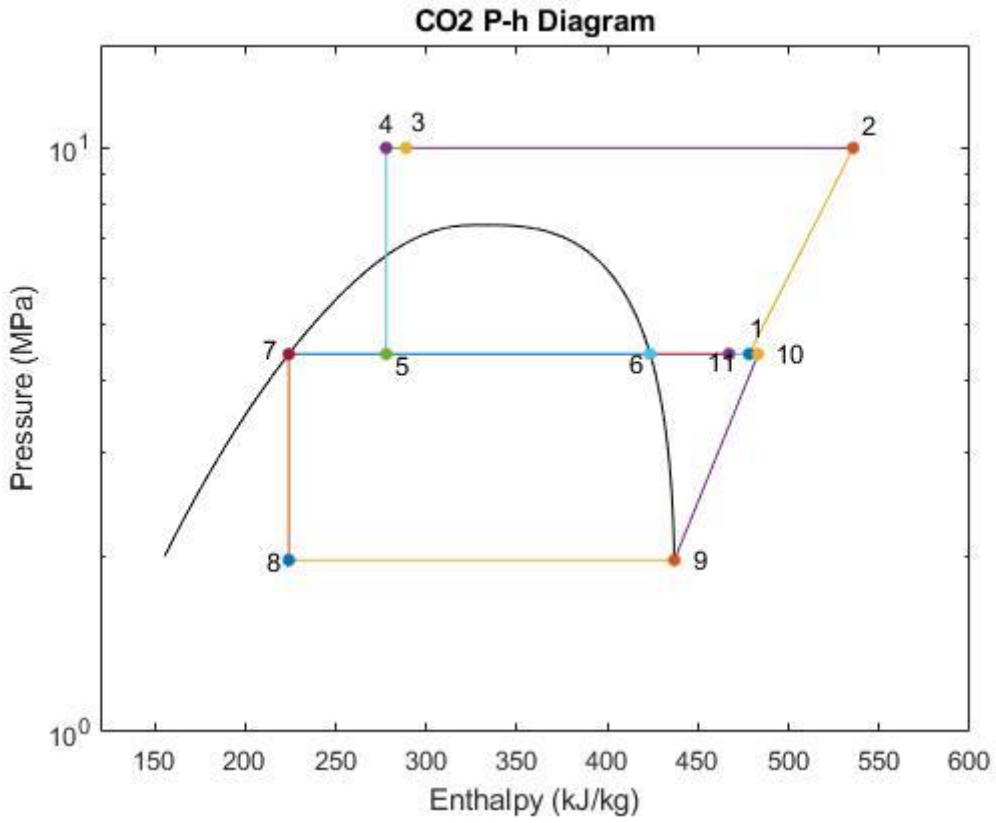

Figure 25-P-h diagram for CO_2 heat pump on BTC cycle with two compressors

Figure 26 displays the performance of BTC cycles at different values of evaporator temperature, when fixing gas cooler pressure P_c and assuming a subcooling degree Δt_c of 0℃. It should be noted that in the present simulations, the selected evaporating temperature range mainly corresponds to the low ambient temperatures of winter season, at which the performance enhancement is an essential requirement for two-stage cycles. It can be observed from Figure 26 that as the evaporating temperature increases, the COP increases as expected.

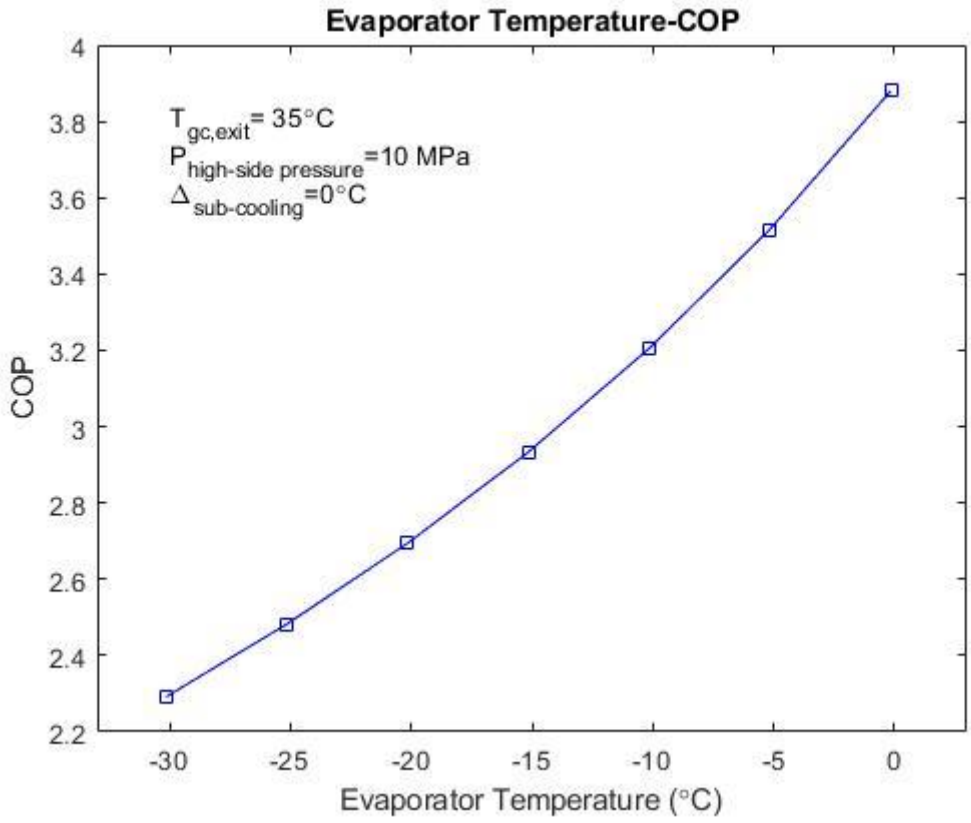

Figure 26-Graph for COP-Evaporator Temperature

It is known that the performance of the CO_2 transcritical cycle is very sensitive to the gas cooler pressure and the maximum COP occurs at an optimal gas cooler pressure. The values of the optimal gas cooler pressure mainly depend on the outlet temperature of the gas cooler, the evaporating temperature, and the performance of the compressor. Similarly, in the case of the two stage CO_2 transcritical cycles, the gas cooler pressure is also an influential parameter to decide the best COP along with the intermediate pressure. Figure 27 shows the variations of the COP and the volumetric heating capacity of BTC cycles with the gas cooler pressure, where the evaporating temperature is taken as $-15℃$, and the gas cooler pressure is varied from 8 to 11.5 MPa. The gas cooler pressure is approximately 8.5 MPa at the given operating conditions for BTC cycle.

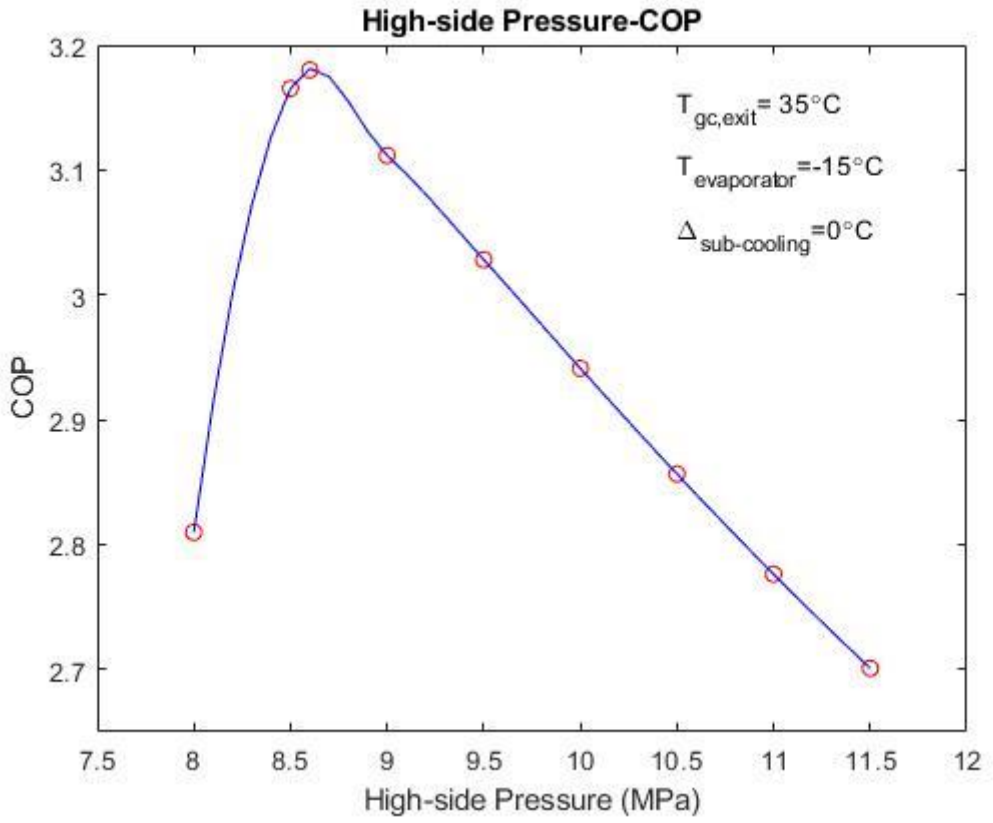

Figure 27-Graph for COP-High-side Pressure

Figure 28 shows the effects of subcooling degree in the internal heat exchanger(IHX) on the performance of BTC cycles. It is observed that in the BTC cycle, the increased subcooling degree in the IHX almost does not affect the cycle performance. This is because in the BTC cycle, the suction vapor of the high pressure (HP) compressor further achieves very large superheat through the IHX based on the superheated mixing vapor stream from the high pressure compressor and flash tank. Consequently, it tends to increase the HP compressor work and heat rejection in the gas cooler as well as the suction specific volume simultaneously. For these reasons, the subcooling degree in the IHX does not finally affect the COP of the BTC cycle.

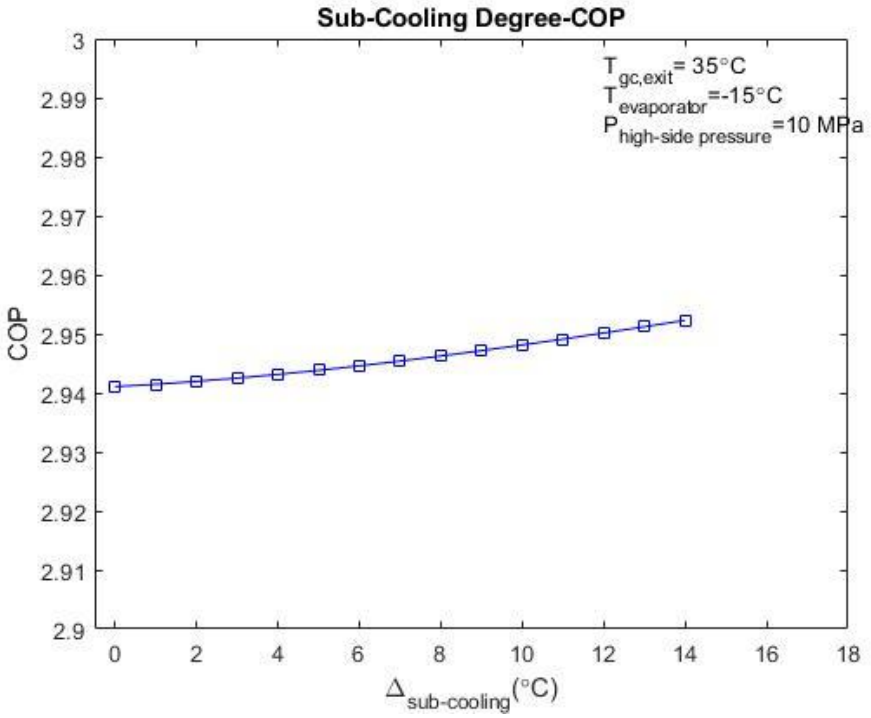

Figure 28-Graph for COP-Sub Cooling Degree

The exergy analysis has been done for different gas cooler temperature in Matlab Coolprop. The maximum exergy loss was observed in the gas cooler, and the minumum exergy loss observed in the flash tank.

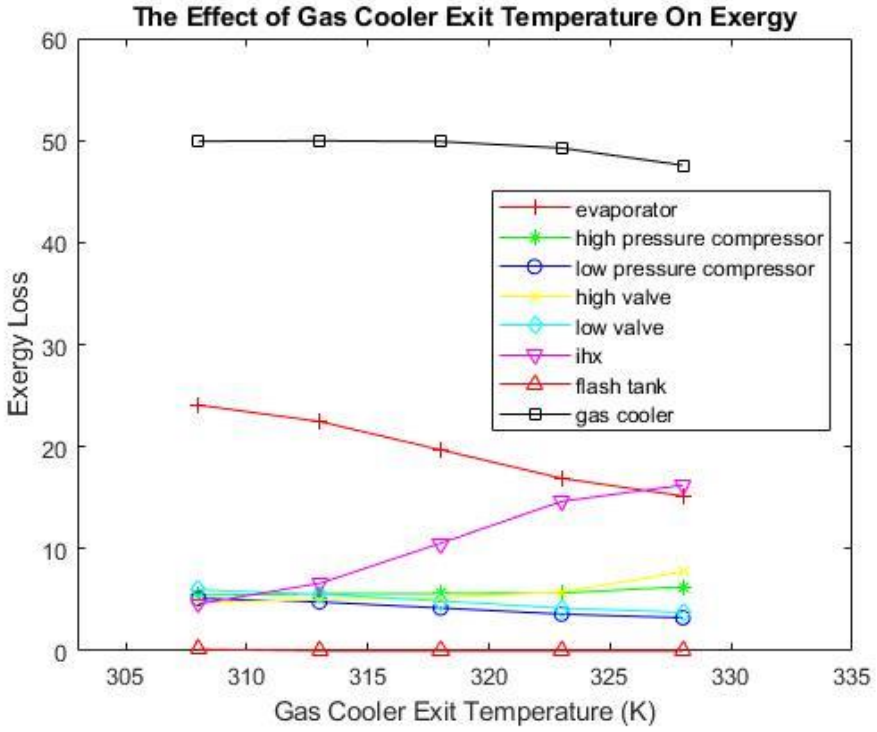

Figure 29-Component Based Exergy Lost Variation With Gas Cooler Temperature

3.4.Results of ESCVI System

The thermodynamic analysis of the ESCVI system has been made using the assumptions mentioned in the previous section with Matlab Coolprop.

The ESCVI system is influenced by many parameters of the cycle. There are some important properties to achieve a higher COP for the CO_2 heat pump. The gas cooler temperature depends on the following parameters;

- The pressure of compressor outlet, so high side pressure
- The characteristics of gas cooler
- The evaporator temperature
- The characteristics of ejector
- The degree of sub-cooling

Figure 30 and 31 shows T-s and P-h diagrams for a ESCVI cycle.

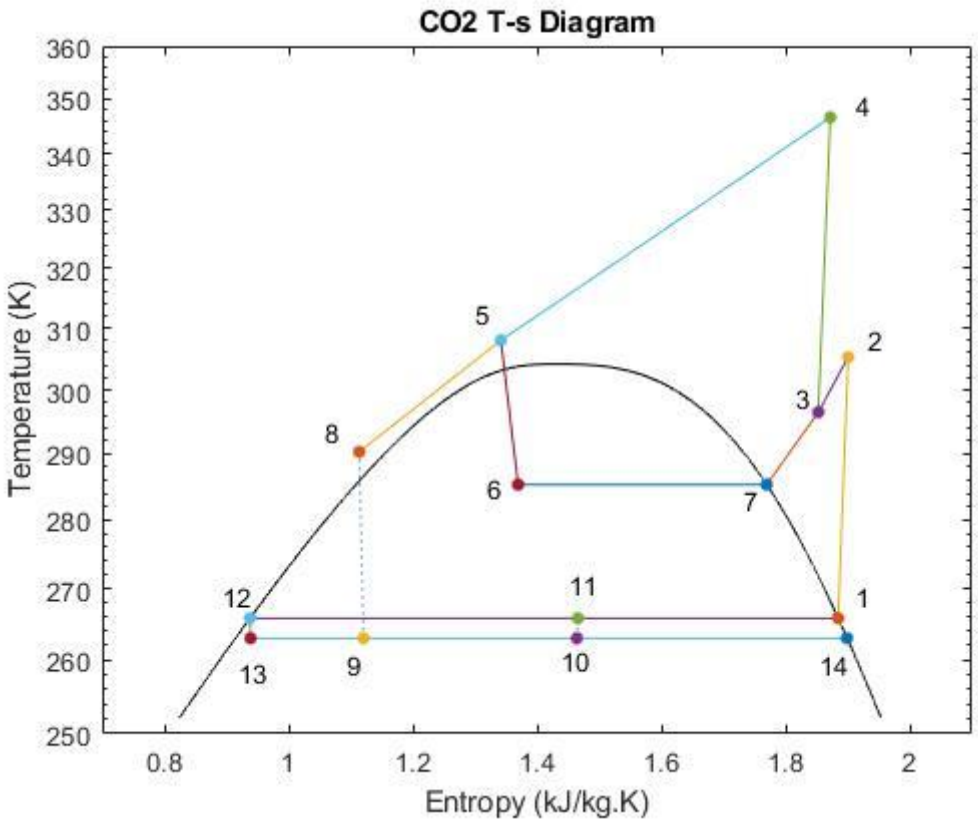

Figure 30- T-s Diagram of ESCVI Cycle

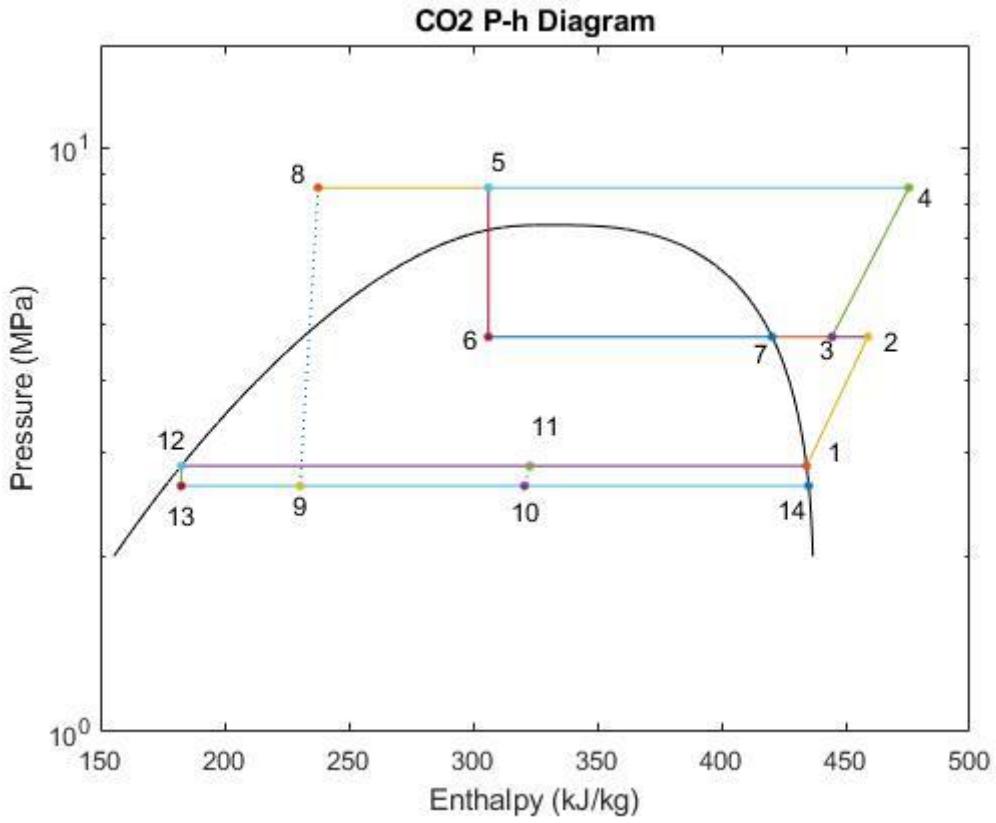

Figure 31- P-h Diagram of ESCVI Cycle

Figure 32 displays the effect of the discharge pressure P_{dis} on the system COP. With the increasing discharge pressure, an optimum discharge pressure value of 8.55 MPa exists at which the system COP reaches the maximum value at 3.671.When the P_{dis} varies from 7.5 to 11.5 MPa under the selected operating condition(the gas cooler temperature at 35℃ and the evaporator temperature at -10℃) the system COP of the ESCVI cycle vary in the range of 2.042-3.671. It has been observed that while the COP value increases with a rapid acceleration when the pressure is between 7.5-8.55 MPa, the COP value continues with a constant decrease after 8.55 MPa pressure.

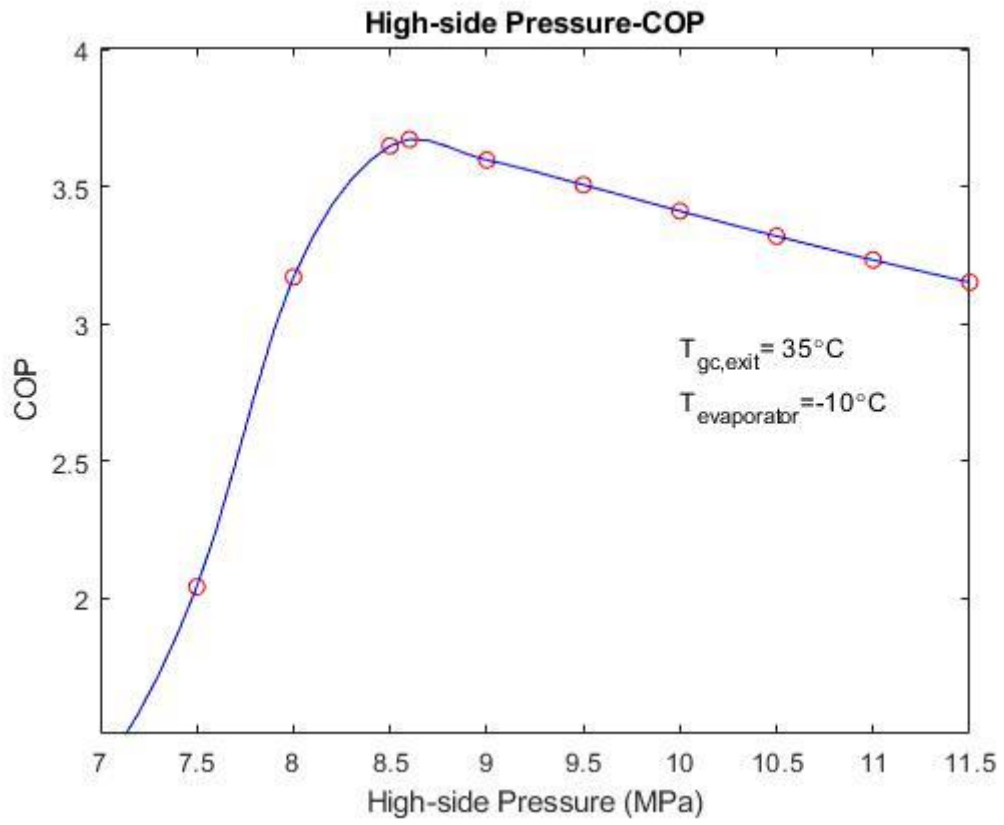

Figure 32- Graph for COP-High-side Pressure

Figure 33 displays the effect of the discharge pressure P_{dis} on the ejector performances including the pressure lift ratio r_P and entrainment ratio μ. It can be observed that the r_P increases with an increase in P_{dis}.When the discharge pressure P_{dis} varies from 7.5 to 11 MPa under the fixed T_{ev} at -10℃ and T_{gc} at 35℃, the r_P increases from 1.0671 to 1.1191, the μ vary in the range of 0.8008-0.7594. The analyses on the Figures 31 and 32 indicate that the ESCVI cycle has considerable thermodynamic improvement potential in the system COP and volumetric heating capacity over the other cycles due to the expansion work recovery effects from the ejector. In addition, it could be found that the discharge pressure significantly affects the system performance. Therefore, the following parametric analyses are all carried out on the optimum discharge pressures, which are accurately obtained.

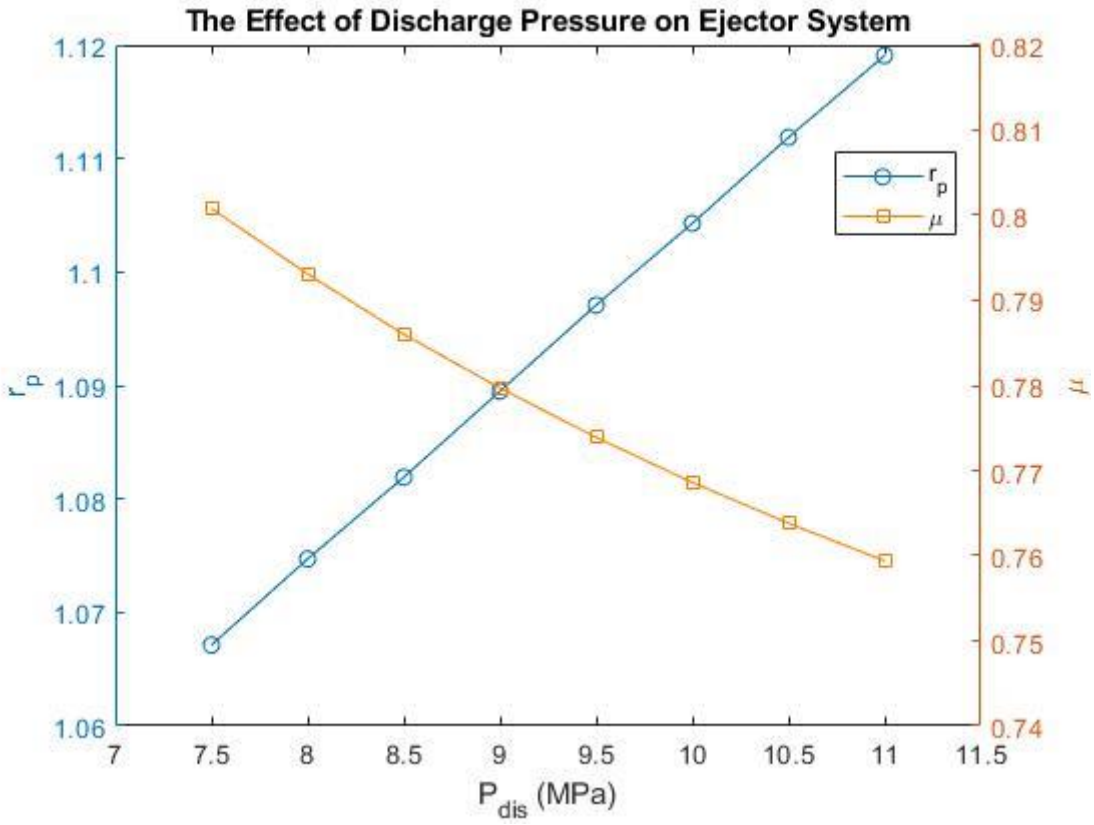

Figure 33-The Effect of Discharge Pressure on Ejector System

Figure 34 shows the variation of system COP with the evaporating temperature for ESCVI cycle at optimum discharge pressures under the given operating conditions; the discharge pressure at 8.55 MPa. It can be observed that the system COP increases as the increasing evaporating temperature for ESCVI cycle, and the ESCVI cycle exhibits higher COP. When the gas cooler exit temperature is fixed at 35 ℃, the evaporating temperature varies from -25 to -5 ℃, the ESCVI cycle shows higher COP. The system COP of the evaporator vary in the range of 2.7234-4.0805 at between -25℃ and -5℃.

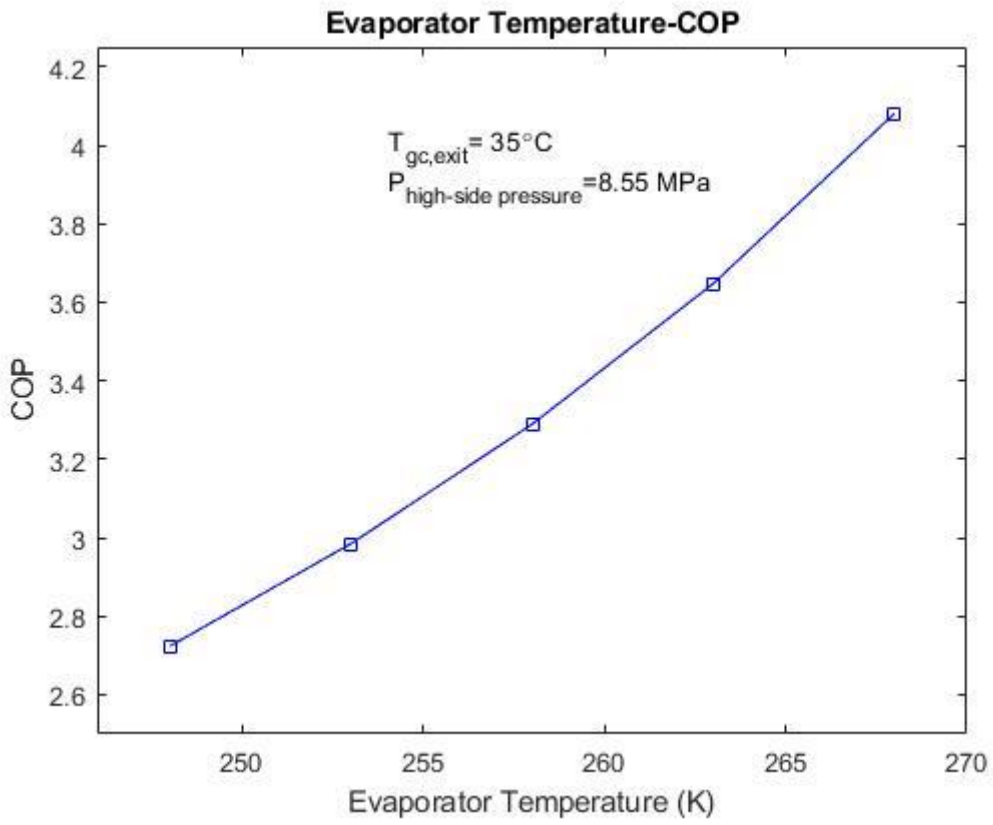

Figure 34-Graph for COP-Evaporator Temperature

Figure 35 presents the effect of evaporating temperature T_{ev} on the ejector performance, and the variations of the pressure lift ratio r_P and entrainment ratio μ with the increasing evaporating temperature. It can be seen that the pressure lift ratio r_P decreases with an increase in the evaporating temperature, because the available expansion ratio (P_8/P_{14}) of the ejector is reduced as the increasing evaporating pressure and the decreasing optimum discharge pressures due to the increasing evaporating temperature. However, both r_P and μ shows slight variation with the increasing T_{ev}. When the T_{ev} varies from -25 to -5 ℃, the r_P shows a slight decrease from 1.0997 to 1.0772 while the μ barely changes. This indicates that the evaporating temperature T_{ev} has little effect on variation of the pressure lift ratio r_P and entrainment ratio μ, and the ejector could steadily operate under the different evaporating temperatures, which is expected for the ejector cycle design in respect to the system operating stability. However, the entrainment ratio(μ) varies from 0.7808 to 0.7862 under the given operating conditions; the discharge pressure at 8.55 MPa and gas cooler exit temperature at 35℃.

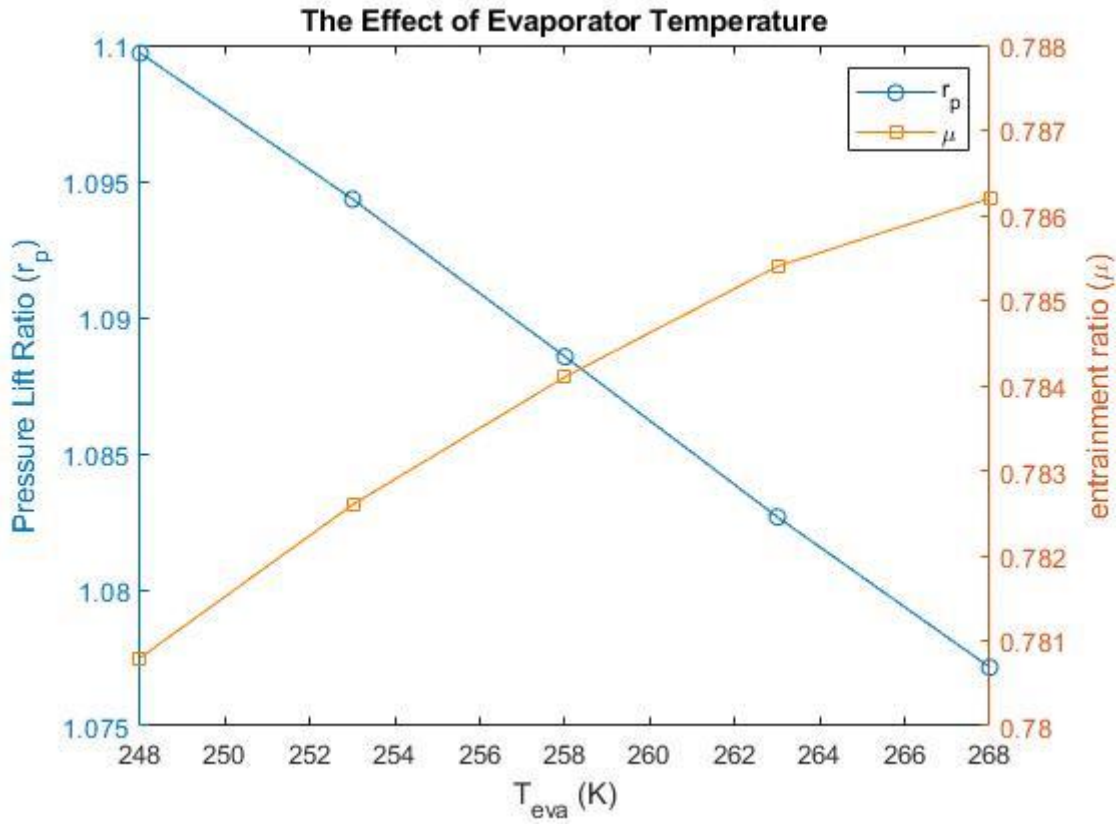

Figure 35-The Effect of Evaporator Temperature on Ejector Performance

The effect of the isentropic efficiencies of the ejector on the pressure lift ratio r_P and entrainment ratio μ under the specialized operating condition(the discharge pressure at 8.55 MPa , gas cooler exit temperature at 35℃ and the evaporator temperature at -10℃) is shown in Figure 36 when the mixing efficiency τ_μ is fixed at 0.95 and the isentropic efficiencies of the nozzle and the diffuser are assumed as $\tau = \tau_\mu = \tau_d$ in the range of 0.7-0.95. It can be observed that r_P and μ with the increasing isentropic efficiencies of the ejector. When τ vary from 0.7 to 0.95, the r_P shows a remarkable increase from 1.0630 to 1.1206, μ barely has slight changes (0.7797 to 0.7802). This means that the suction pressure of the compressor can be enhanced with the assistance of the ejector and the entrainment ratio maintains slight variation, which are expected for the compressor work saving and system steady operation.

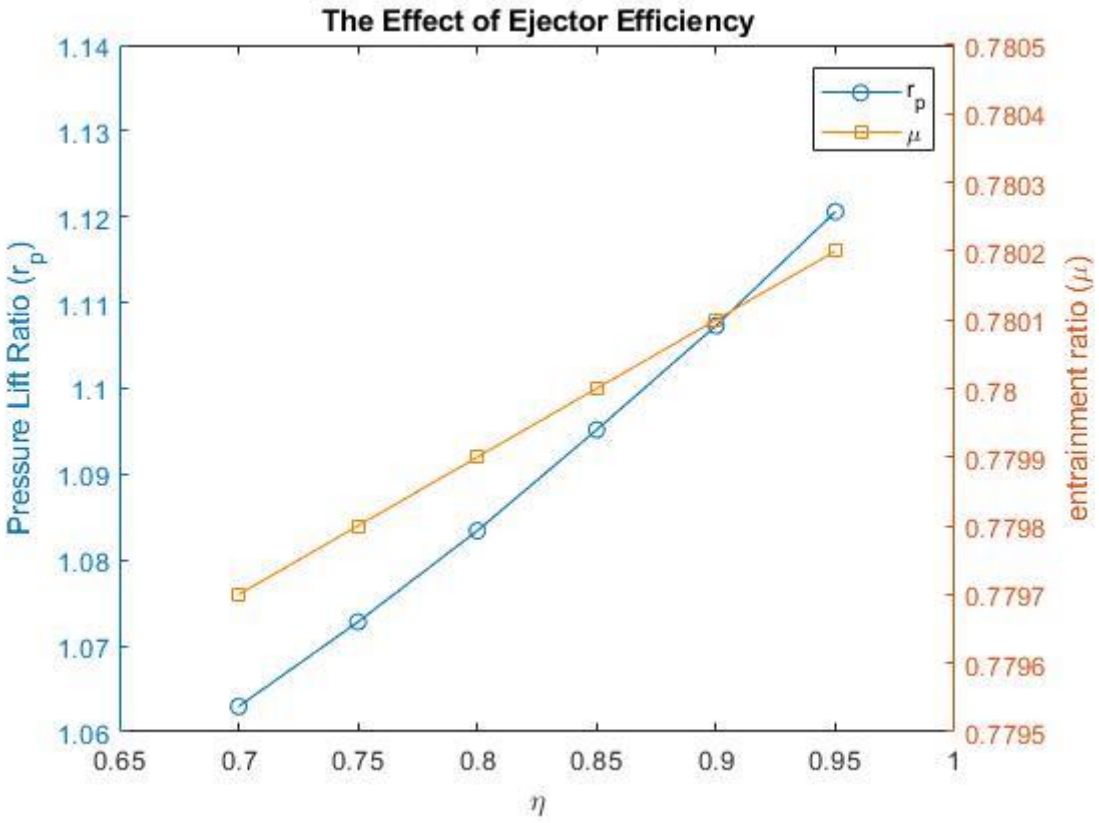

Figure 36-The Effect of Ejector Efficiency

The graph shown in Figure 37 shows the ratio of entrainment ratio (μ) to COP under the specified conditions. Discharge pressure varies between 7-11.5 MPa, while entrainment ratio(μ) varies between 0.8096-0.7553. While the entrainment ratio increases linearly between 0.7553 and 0.7867, it is observed that it decreases rapidly between 0.7867 and 0.8096. The COP value varies between 1.3713-3.6476. Thus, the maximum COP value is seen as 3.6476.

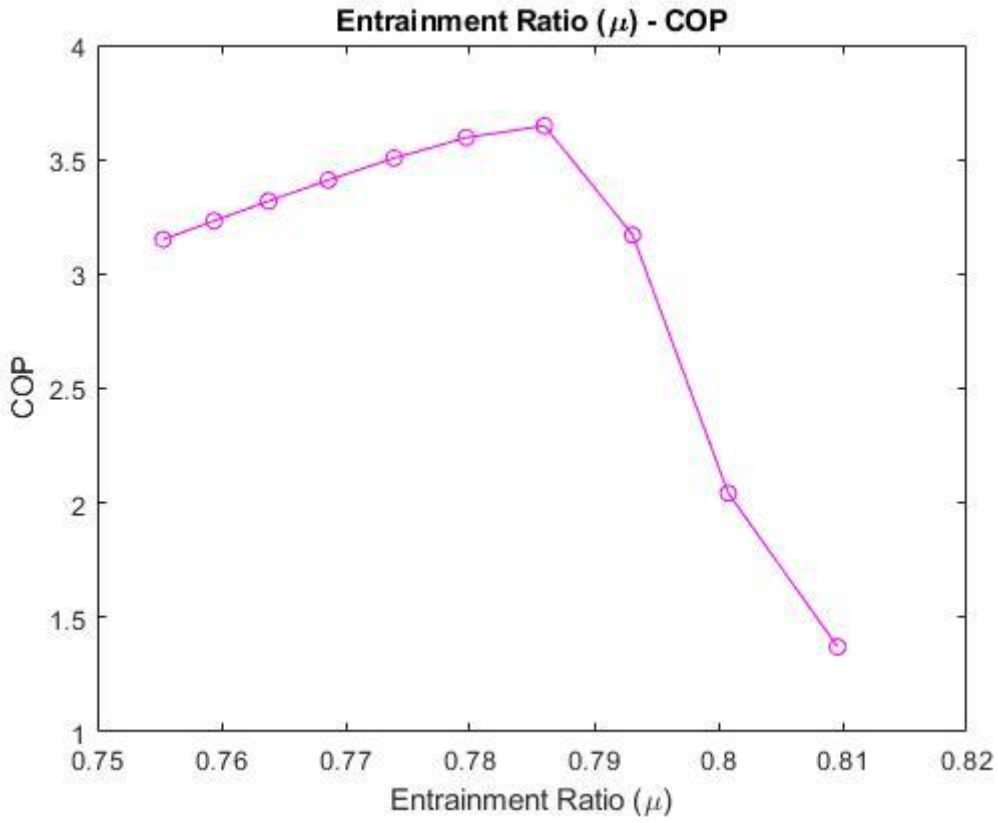

Figure 37-Graph for COP-Entrainment Ratio(μ)

The graph shown in Figure 38 shows the ratio of pressure lift ratio to COP under the specified conditions. Discharge pressure varies between 7-11.5 MPa, while the pressure lift ratio varies between 1.0599-1.1263. While the COP ratio increases rapidly between 1.0599 and 1.0819, it is observed that it decreases linearly between 1.0819 and 1.1263. The COP value varies between 1.3713-3.6476. Thus, the maximum COP value is seen as 3.6476.

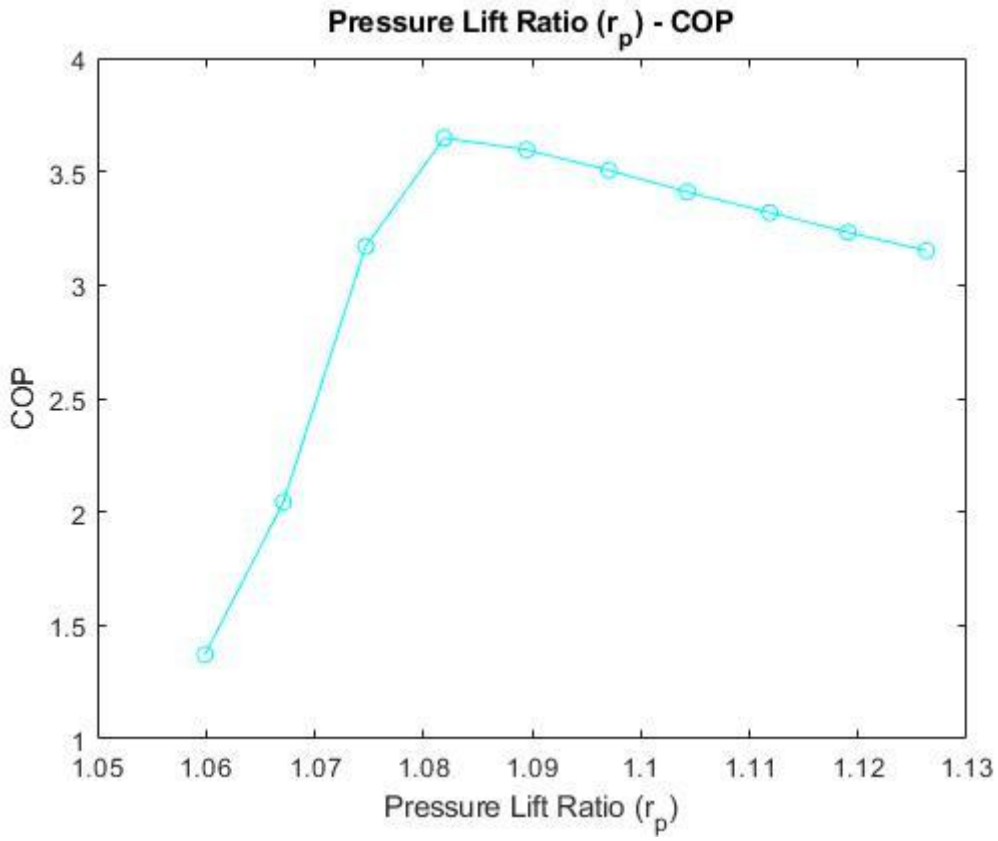

Figure 38-Graph for COP versus Pressure Lift Ratio(r_P)

The exergy analysis has been made for different evaporator temperature in Matlab Coolprop. The maximum exergy loss was observed in the gas cooler cause of heat loss to the part of water. The minimum exergy loss observed in the flash tank, due to there is no heat and energy loss in the flash tank.

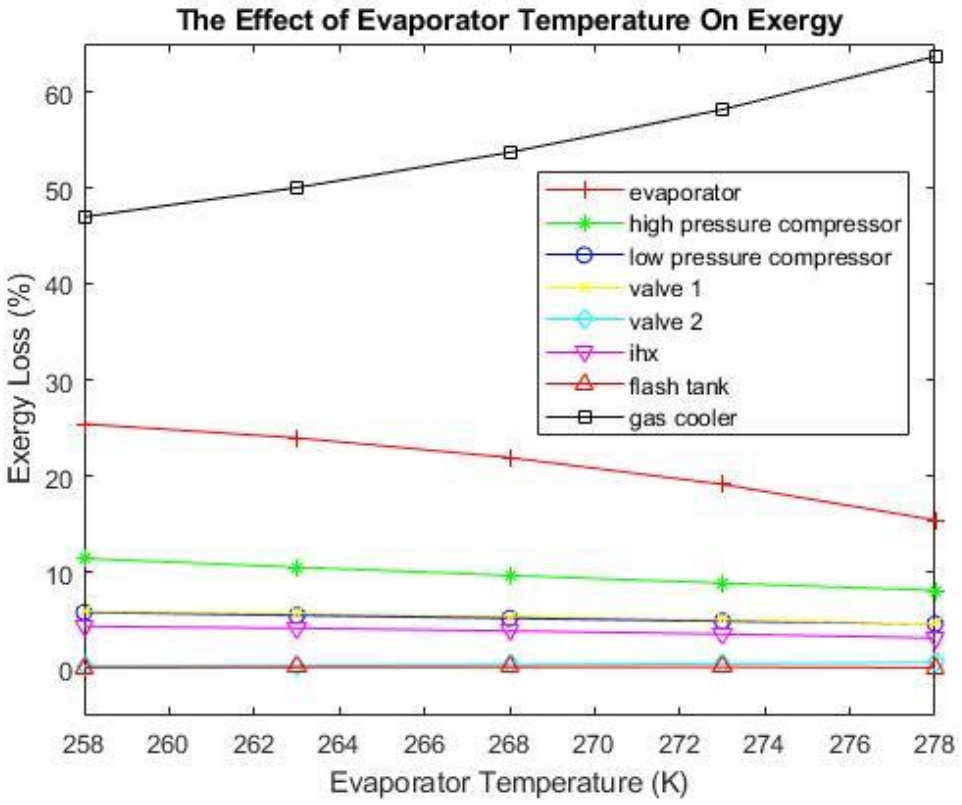

Figure 39-The Effect of Evaporator Temperature on Exergy

Table 6-Evaporator Temperature Effect on The Exergy Destruction

	258 K	263 K	268 K	268 K	273 K
Evaporator (kW)	26.4813	20.9368	15.8774	11.3154	7.2736
High Pressure Compressor (kW)	11.9717	9.2142	7.0111	5.2479	3.8361
Low Pressure Compressor (kW)	6.0643	4.8053	3.7586	2.8917	2.1748
Valve 1 (kW)	6.2047	4.9784	3.9134	2.9893	2.1915
Valve 2 (kW)	0.2143	0.2283	0.2432	0.2581	0.2720
Internal Heat Exchanger (kW)	4.5494	3.6218	2.8048	2.0925	1.4794
Flash Tank (kW)	0.2459	0.1980	0.1580	0.1191	0.0839
Ejector (kW)	16.0582	13.3574	10.8648	8.5692	6.4760
Gas Cooler (kW)	49.3463	43.9829	39.1109	34.5904	30.2999
Overall System (kW)	121.1360	101.3230	83.7422	68.0735	54.0873

3.5.Results of ETC System

The diagram in the figure shows the solving procedure of the BTC cycle.

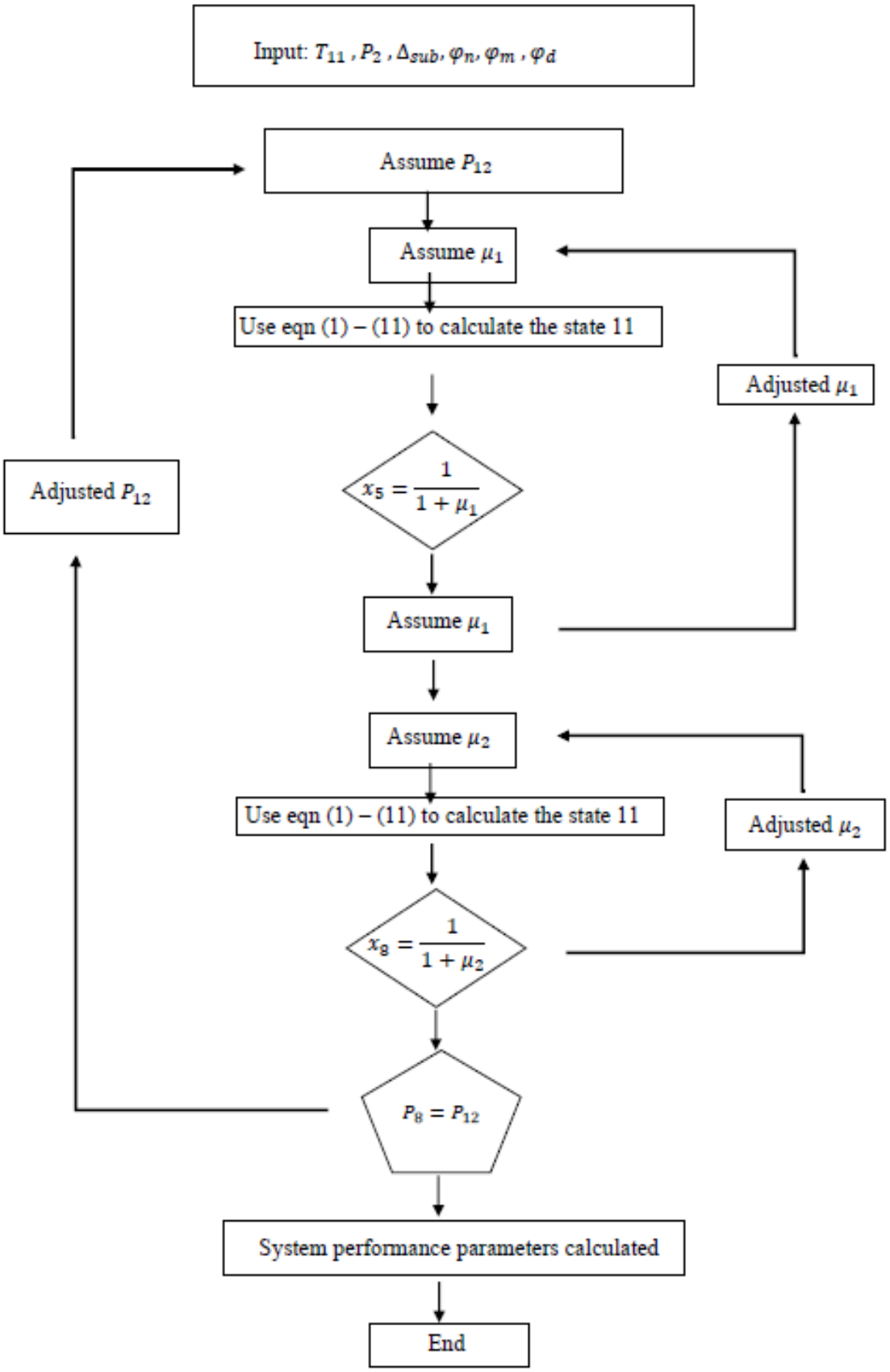

Figure 40-Solving Procedure of The BTC Cycle

The ETC system has been made its thermodynamic analysis using the assumptions mentioned in the previous section with Matlab Coolprop.

The ETC system is influenced by many parameters of the cycle. There are some important properties to achieve a high COP for the CO_2 heat pump. The gas cooler temperature depends on the following parameters;

- The pressure of compressor outlet, so high side pressure
- The characteristics of gas cooler
- The evaporator temperature
- The characteristics of HP and LP ejectors
- The degree of sub-cooling

Figure 41 and 42 shows T-s and P-h diagrams for a ETC cycle.

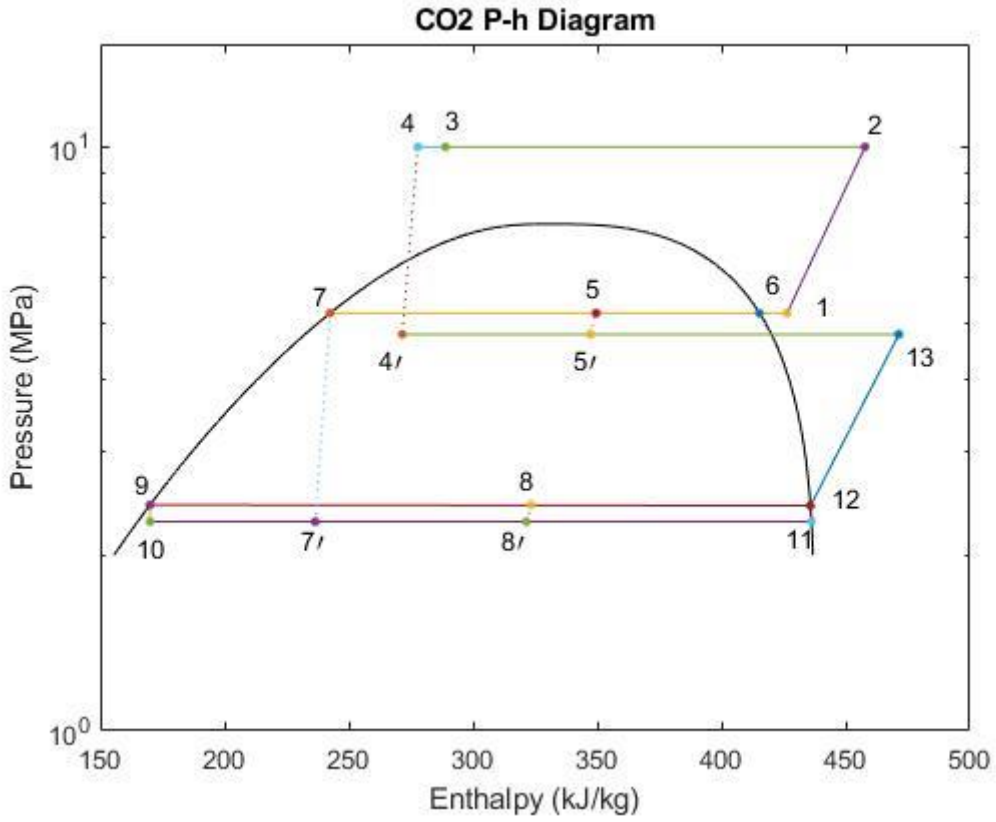

Figure 41-P-h Diagram of ETC Cycle

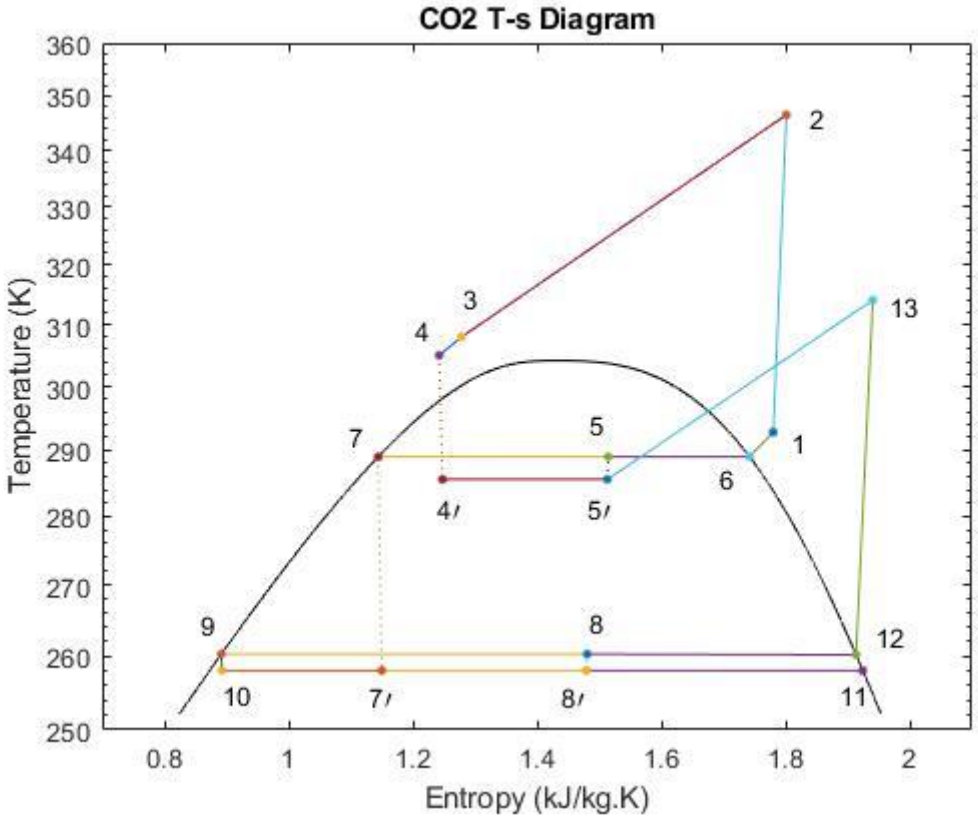

Figure 42-T-s Diagram of ETC Cycle

The efficiency of ejectors may vary with many factors, such as operating conditions and ejector geometry. Thus, the influence of ejector efficiency on the ETC cycle performance is firstly examined. Figure 43 shows the dependence of the COP_h on the overall isentropic ejector efficiency τ_e, where the gas cooler pressure is 10 MPa, the evaporating temperature is taken as -15 ℃ and the subcooling degree Δ_{sub} is 0℃. Note that the definition of the overall ejector efficiency is introduced here based on $\tau_e = \tau_n \tau_m \tau_d$. It can be seen from Figure 43 that the COP_h present a rising trend with the increased ejector efficiency. When the τ_e is varied from 0.412 to 0.625, the COP_h is increased by 2.92%. Overall, the ETC cycle performance increases for higher ejector efficiency. Thus, increasing ejector efficiency including the individual component efficiencies of an ejector should be expected for the ETC cycle. Considering this case, the ejector isentropic efficiencies are assumed to be τ_n = 0.8, τ_m = 0.95 and τ_d = 0.8 in the following simulations for simplicity.

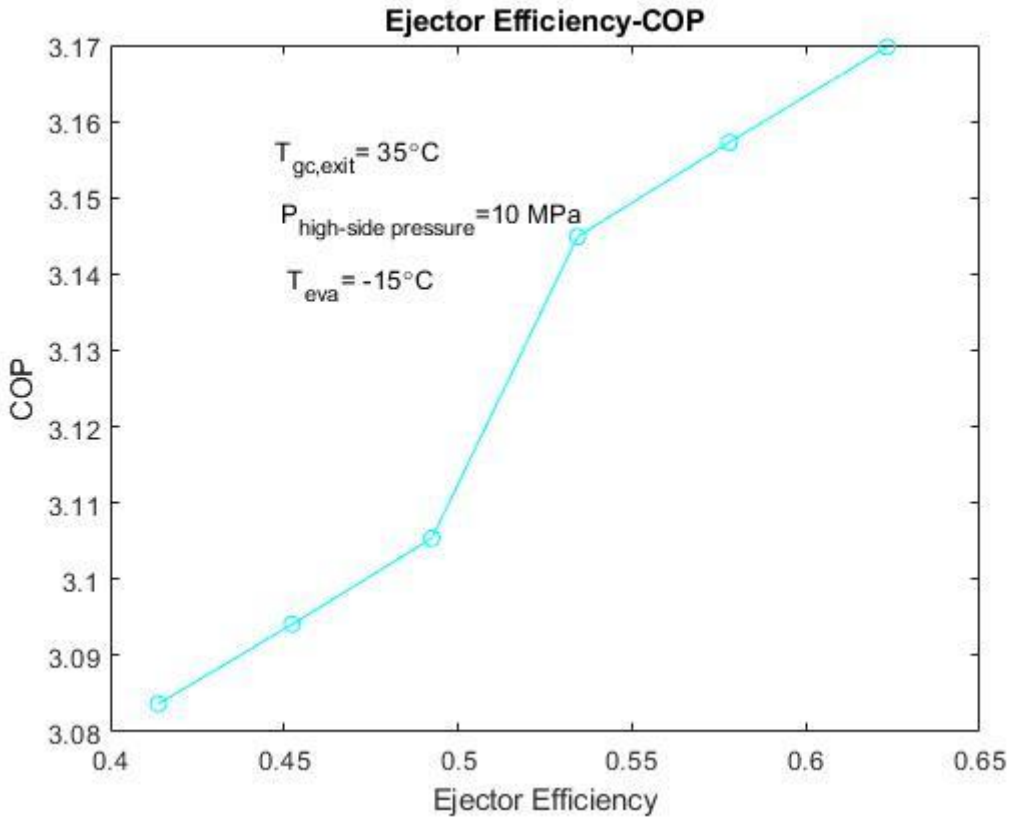

Figure 43-The Graph of COP-Ejector Efficiency

Figure 44 displays the performance of the ETC cycle at different values of T_{eva} , when fixing gas cooler pressure P_c at 10 MPa and assuming a subcooling degree Δ_{sub} of 3℃. It can be observed from Figure 44 that as the evaporating temperature increases, the COP_h increases as expected. For the operating conditions considered, When the evaporator temperature is varied from 238K to 273K, the COP_h is increased by 71.3% as can be seen in Figure 44. Obviously, the performance enhancement potential of the ETC cycle is due to the double ejectors, which efficiently reduce the inherently large throttling losses and enable the suction pressures of two compressors to be increased.

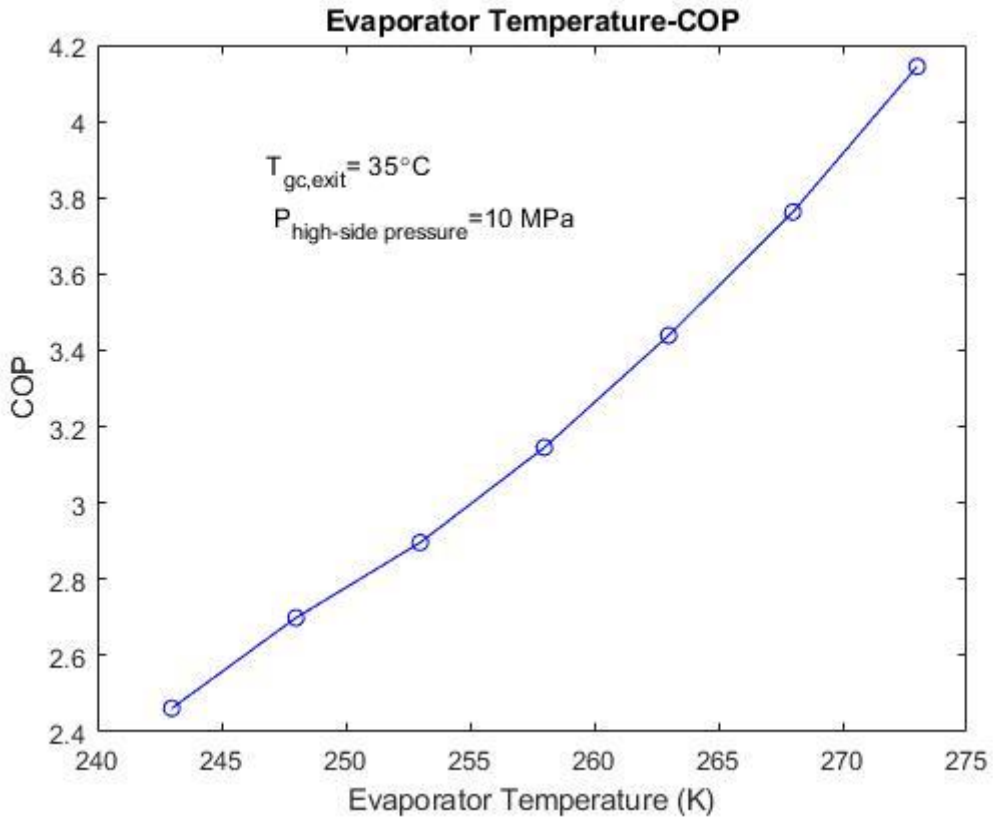

Figure 44-Graph of COP-Evaporator Temperature

Figure 45 shows the performance of the two ejectors, including the entrainment ratio and pressure lifting ratio, at gas cooler pressure P_c at 10 MPa and assuming a subcooling degree Δ_{sub} of 3℃ operating conditions. It can be seen that for the HP ejector, the pressure lifting ratio increases with decreasing the evaporating temperature, while the entrainment ratio varies inversely. The pressure lift ratio of the LP ejector has a similar trend for the entire range of evaporating temperature. In addition, its entrainment ratio has a small variation over the evaporating temperature range. Overall, there is a sharp increase in the pressure lifting ratio for the HP ejector compared to the LP ejector especially at lower evaporating temperatures. The reason is that when the evaporating temperature is reduced, the corresponding intermediate pressure is also lowered. This means more expansion work can be recovered by the HP ejector, which yields a higher pressure lifting ratio. On the other hand, the entrainment ratio is decreased due to the higher pressure lifting ratio, which is the main operating conditions of an ejector. Under the above operating conditions, the pressure lifting ratios in the HP ejector range from 1.064 to 1.121 and in the LP ejector from 1.061 to 1.082. Thus, the HP ejector in the ETC cycle offers a better function of recovering expansion work from throttling process and it becomes imperative to improve overall cycle performance.

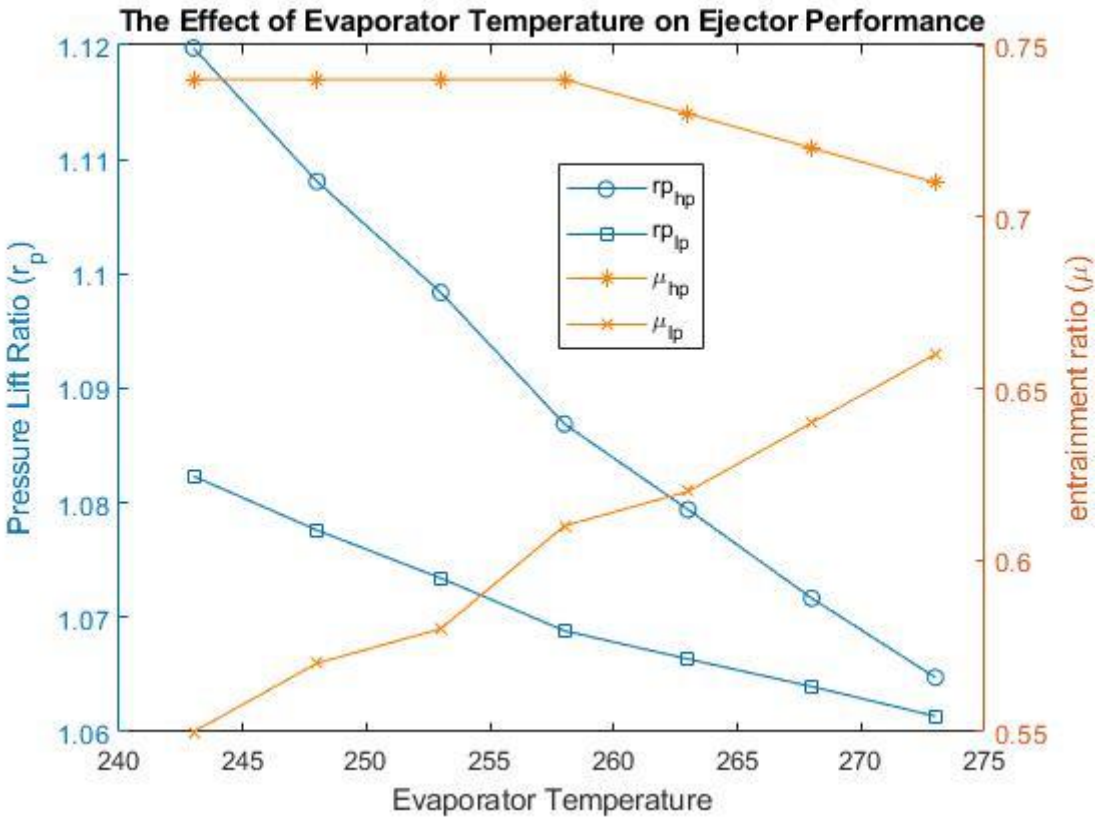

Figure 45-Graph of The Effect of Evaporator Temperature on Ejector Performance

Figure 46 shows the variations of the COP_h of the ETC cycle with the gas cooler pressure, where the evaporating temperature is taken as -15℃, and the gas cooler pressure is varied from 8 to 11.5 MPa. It can be found that there is an optimum gas cooler pressure for the ETC cycle, as gas cooler pressure increases. The optimum gas cooler pressure value is approximately 8.55 MPa at the given operating conditions. This also implies that the optimum gas cooler pressure in the two-stage CO_2 transcritical cycle be nearly unaffected by the use of double ejectors, even though it leads to an improvement of the COP_h.

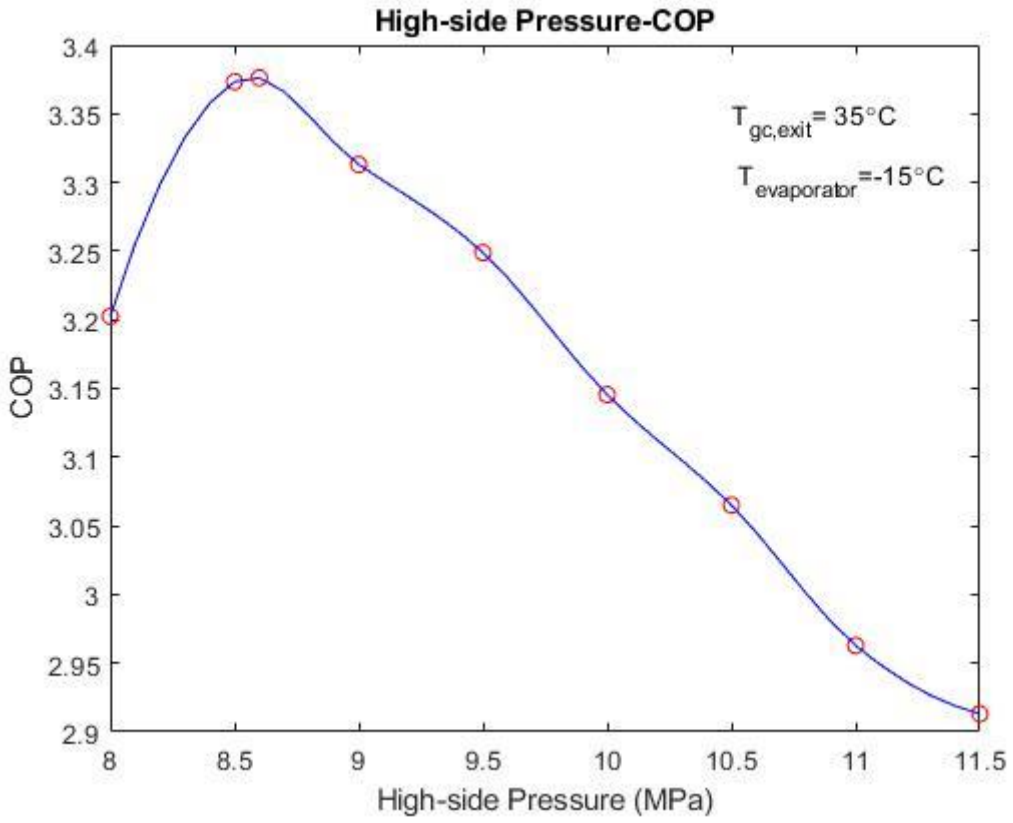

Figure 46-Graph of COP-High-side Pressure

The performance of two ejectors in the ETC cycle is presented in Figure 47 at different gas cooler pressures. It is again seen that the HP ejector exhibits the higher work recovery potential and has a positive effect on the cycle performance improvements. The highest ejector pressure lifting ratios of the HP ejector are achieved for the lowest gas cooler pressures. This can be attributed to the fact that the expected increase of the pressure lifting ratio with further increasing gas cooler pressure could not be obtained due to the increasing entrainment ratio as shown in Figure 47. The simulation results show that the pressure lifting ratio of the HP ejector varies from 1.091 to 1.094 for the given range of gas cooler pressures, while the pressure lifting ratio of the LP ejector is from 1.05 to 1.08. Overall, although the HP ejector plays an important role in the COP_h improvement of a two-stage CO_2 transcritical cycle, the two ejectors can be simultaneously used to gain much higher value of the COP_h.

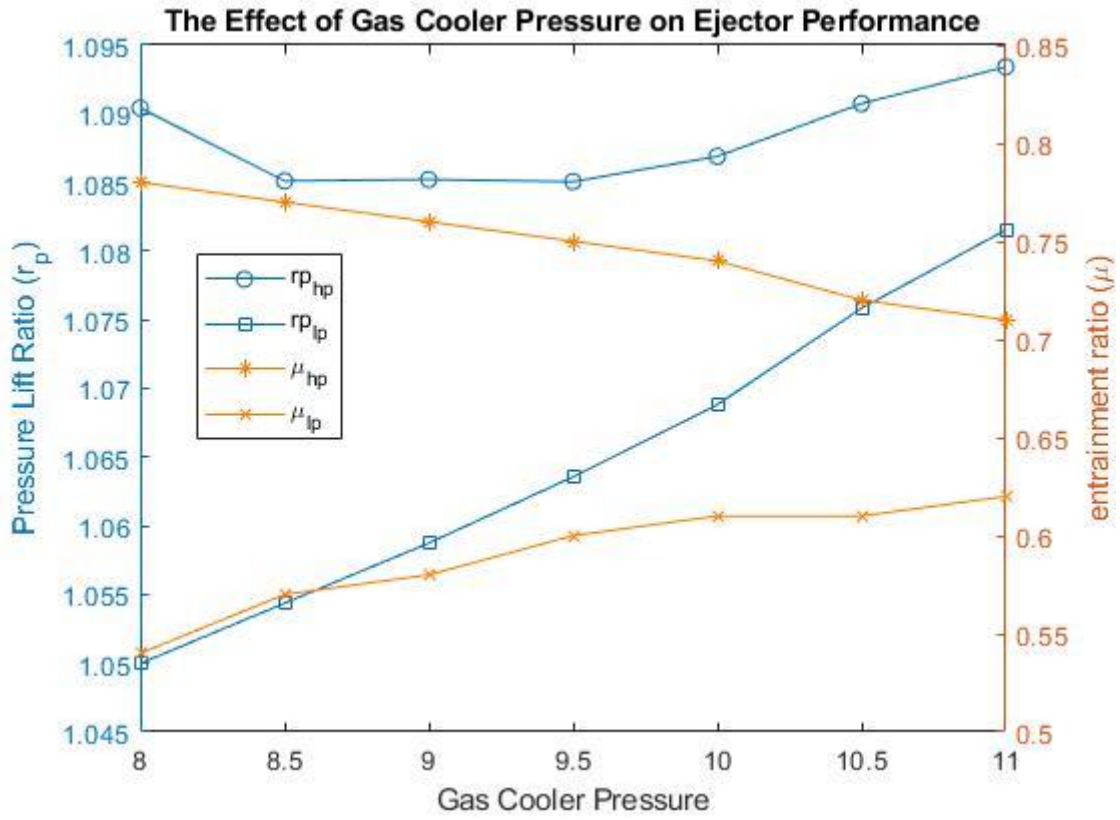

Figure 47-Graph of The Effect of Gas Cooler Pressure on Ejector Performance

It was observed that the most efficient cycle is ETC as a result of the thermodynamic analysis.

4.OPTIMIZATION STUDIES

4.1. BTC Cycle

Two variable optimization studies to optimize the BTC system performance are performed using MATLAB software. The evaporator temperature (T_{eva},K) and the gas cooler pressure (P_{gc}) are chosen to be the independent variables while the subcooling degree (Δ_{sub}) are kept constant at 5℃. The figure 48 represents a three-dimensional surface plot of COP with evaporator temperature and gas cooler pressure.

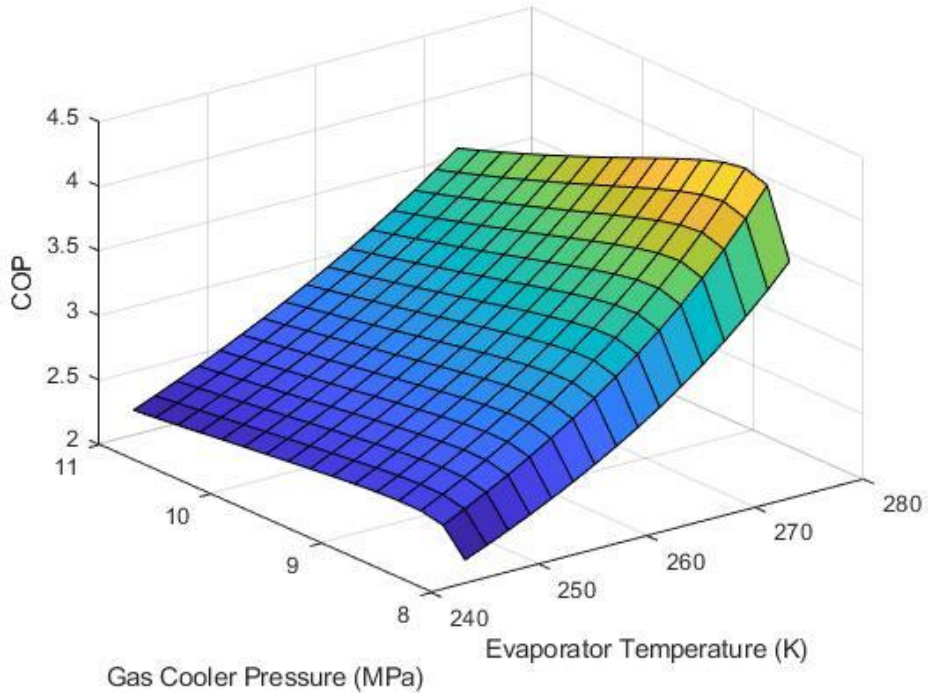

Figure 48-Surface Plot of COP on BTC Cycle

The figure 49 represents a contour plot of COP with evaporator temperature and gas cooler pressure, contour plotting has 0.2 levelstep.

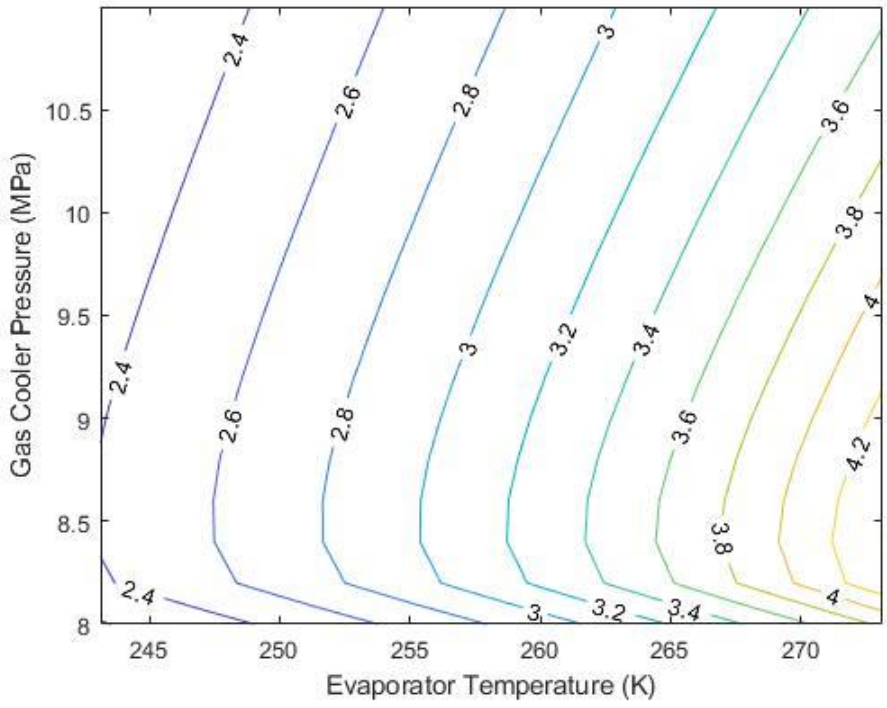

Figure 49- Contour Plot of COP on BTC Cycle

It was created a plane corresponding to datas using lineer regression analysis as shown figure 50.

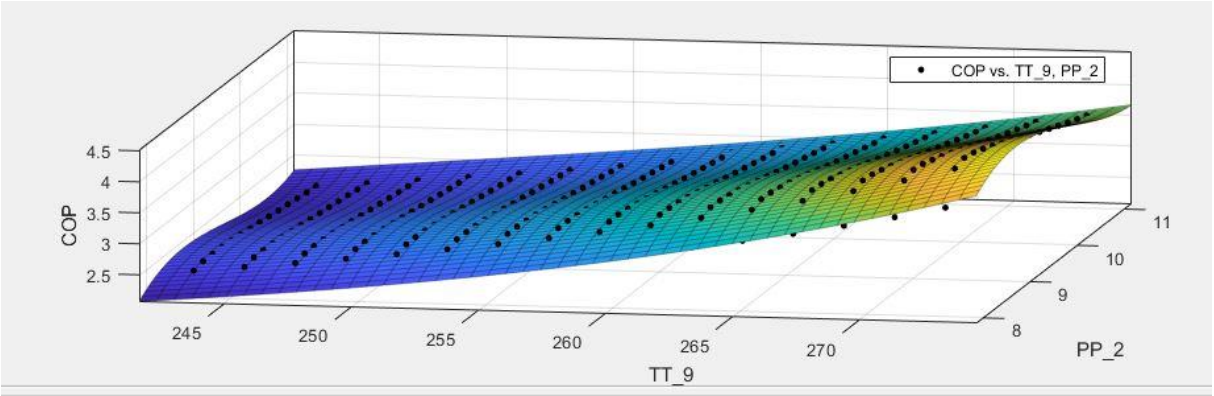

Figure 50-Lineer Regression Analysis of BTC Cycle

The correlation obtained depending on the two parameters examined is shown below:

$$COP = -90.82 + (0.9957\ T_{eva}) + (3.256\ P_{gc}) - (0.007009\ T_{eva}^2) + (0.1457\ T_{eva}\ P_{gc}) - (2.178\ P_{gc}^2) + (0.00001262\ T_{eva}^3) - (0.000207\ T_{eva}^2\ P_{gc}) - (0.00236\ T_{eva}\ P_{gc}^2) + (0.09469\ P_{gc}^3)$$

$$R^2 = 0.9897$$

The evaporation temperature ranges from 240K to 270K. In addition, the gas refrigerant pressure (P_{gc}) is varied from 8MPa to 12MPa in 0.5MPa increments.

It was determined the optimum operating conditions of BTC cycle with optimization studies. As the evaporator temperature increases, the COP of the BTC cycle increases and the optimum COP occurs at the evaporator temperature of 270 K. Besides, the gas cooler pressure, on the other hand, reaches the maximum COP value at approximately 8.55 MPa, and then decreases continuously.

4.2.ESCVI Cycle

Two variable optimization studies to optimize the ESCVI cycle performance are performed using MATLAB software. The evaporator temperature (T_{eva},K) and the gas cooler pressure (P_{gc}) are chosen to be the independent variables while the subcooling degree (Δ_{sub}) are kept constant at 5℃. The figure 51 represents a three-dimensional surface plot of COP with evaporator temperature and gas cooler pressure.

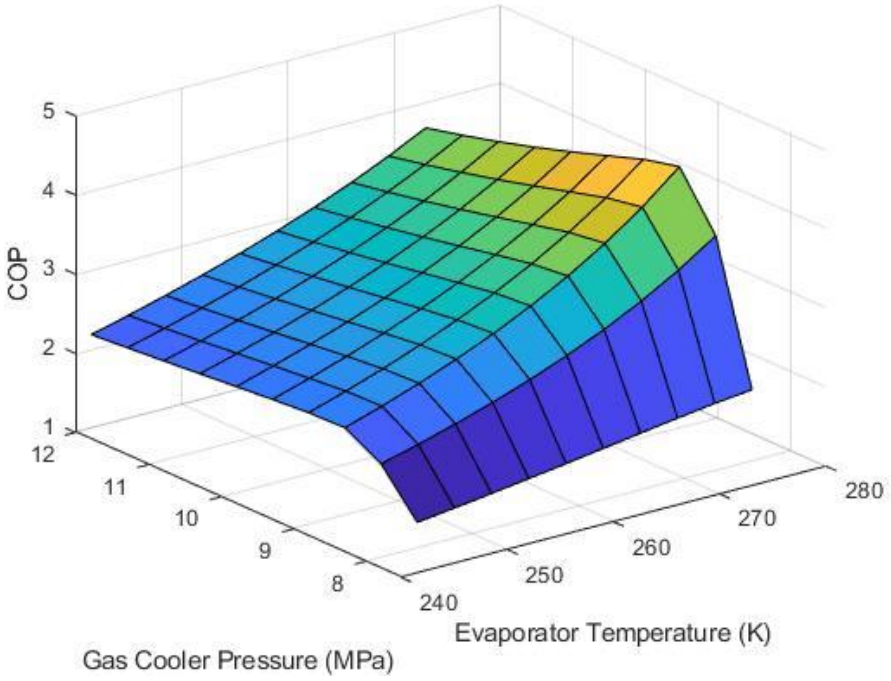

Figure 51- Surface Plot of COP on ESCVI Cycle

The figure 52 represents a contour plot of COP with evaporator temperature and gas cooler pressure, contour plotting has 0.3 levelstep.

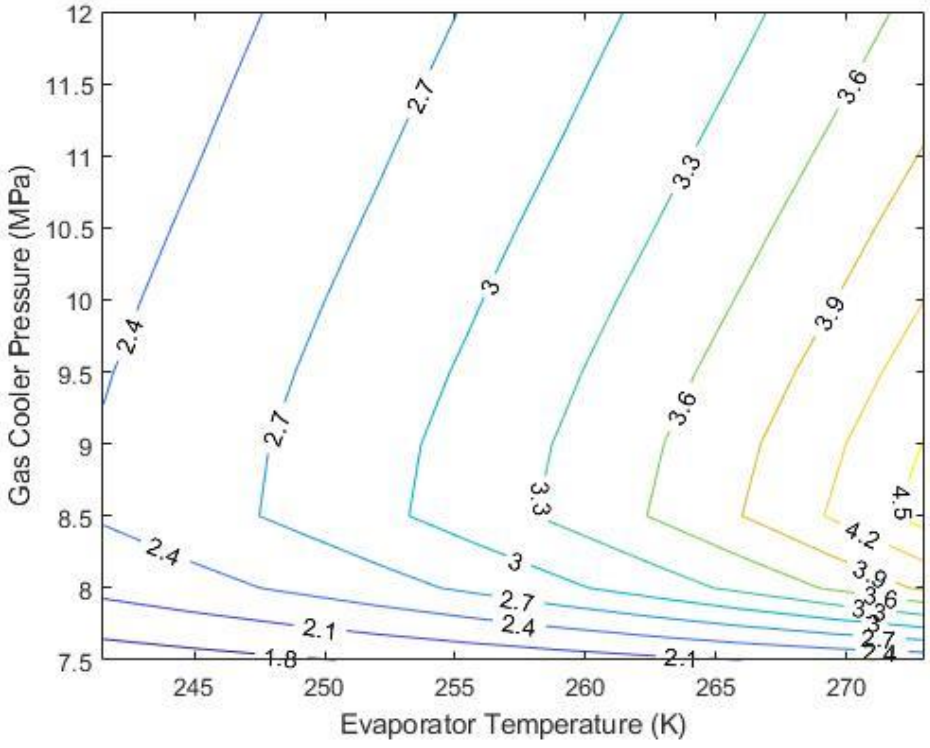

Figure 52- Contour Plot of COP on BTC Cycle

It was created a plane corresponding to datas using lineer regression analysis as shown figure 53. A fourth-order equation was used for a more accurate regression analysis in the ESCVI cycle.

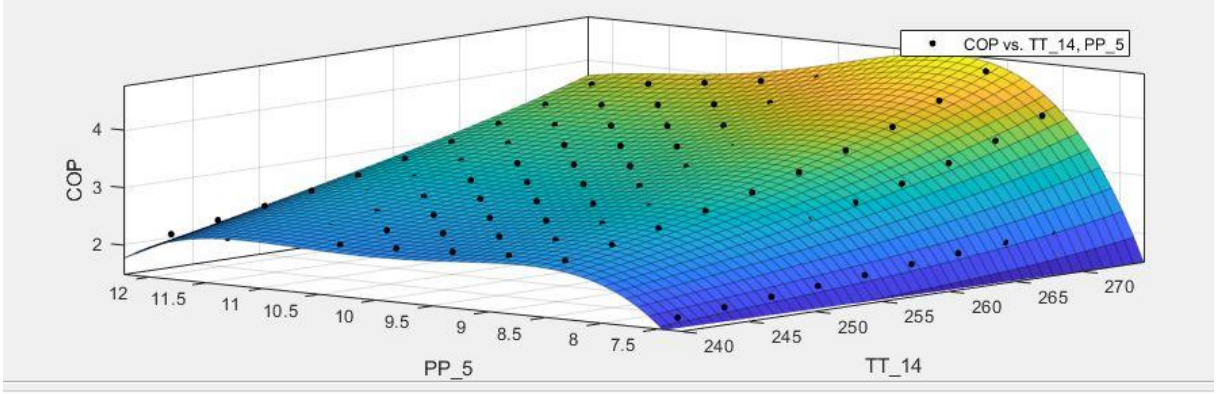

Figure 53- Lineer Regression Analysis of ESCVI Cycle

The correlation obtained depending on the two parameters examined is shown below:

$$COP = 243.2 - (5.902\,T_{eva}) + (45.77\;P_{gc}) + (0.03903\,T_{eva}^2) - (0.1198\,T_{eva}\,P_{gc}) - (5.336\;P_{gc}^2) - (0.0001395\,T_{eva}^3) + (0.002314\,T_{eva}^2\,P_{gc}) - (0.0444\,T_{eva}\,P_{gc}^2) + (0.7124\,P_{gc}^3) + (1.47x10^{-07}T_{eva}^4) + 1.47x10^{-07}T_{eva}^4 - (0.0001191\,T_{eva}^2 P_{gc}^2) + (0.003428\,T_{eva}\,P_{gc}^3) - (0.03848\,P_{gc}^4)$$

$$R^2 = 0.9934$$

The evaporation temperature ranges from 240K to 270K. In addition, the gas refrigerant pressure (P_{gc}) is varied from 8MPa to 12MPa in 0.5MPa increments.

It was determined the optimum operating conditions of ESCVI cycle with optimization studies. As the evaporator temperature increases, the COP of the ESCVI cycle increases and the optimum COP occurs at the evaporator temperature of 270 K. Besides, the gas cooler pressure, on the other hand, reaches the maximum COP value at approximately 8.55 MPa, and then decreases continuously.

4.3.ETC Cycle

Two variable optimization studies to optimize the ETC cycle performance are performed using MATLAB software. The evaporator temperature (T_{eva},K) and the gas cooler pressure (P_{gc}) are chosen to be the independent variables while the subcooling degree (Δ_{sub}) are kept constant at 5℃. The figure 54 represents a three-dimensional surface plot of COP with evaporator temperature and gas cooler pressure.

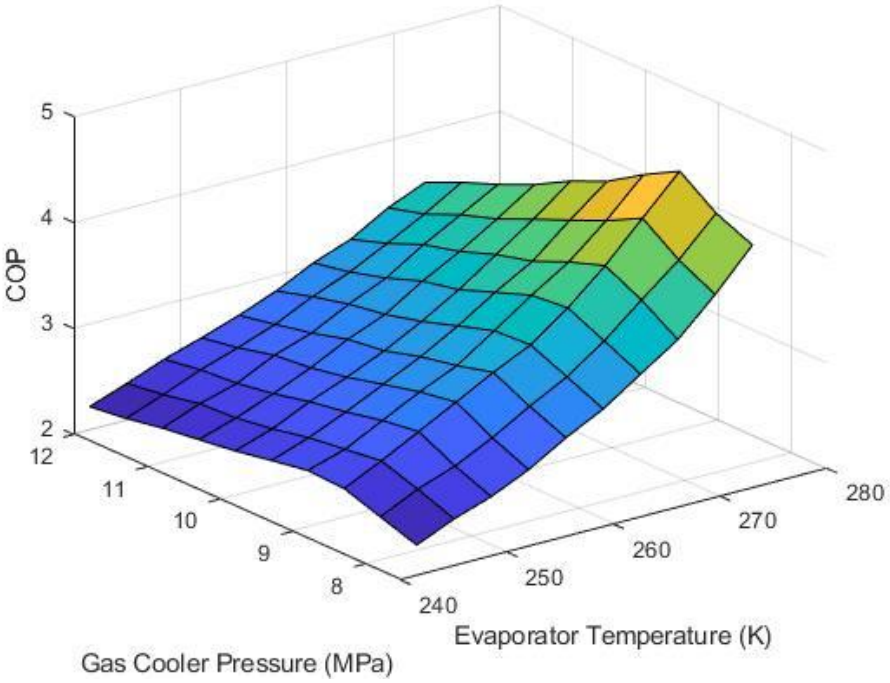

Figure 54- Surface Plot of COP on ETC Cycle

The figure 55 represents a contour plot of COP with evaporator temperature and gas cooler pressure, contour plotting has 0.2 levelstep.

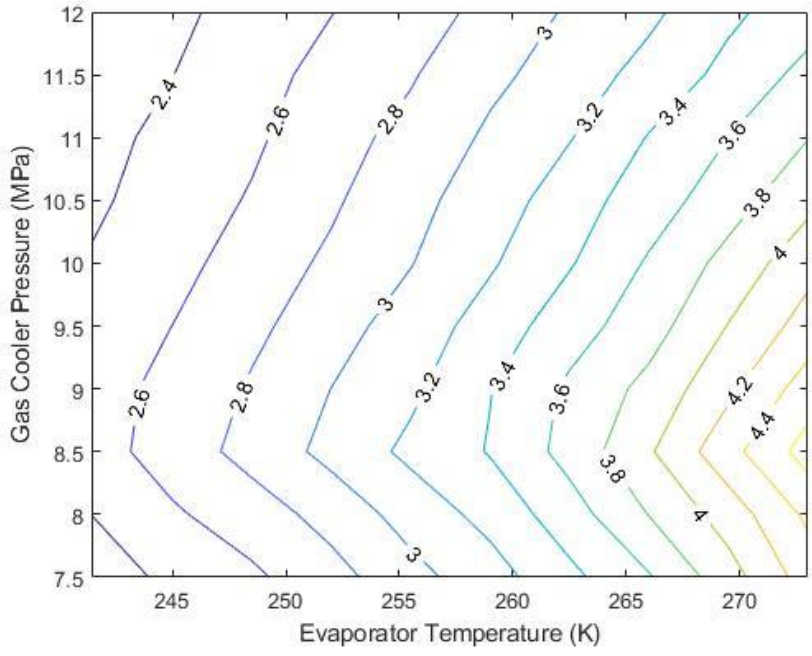

Figure 55- Contour Plot of COP on ETC Cycle

It was created a plane corresponding to datas using lineer regression analysis as shown figure 56. A fourth-order equation was used for a more accurate regression analysis in the ETC cycle.

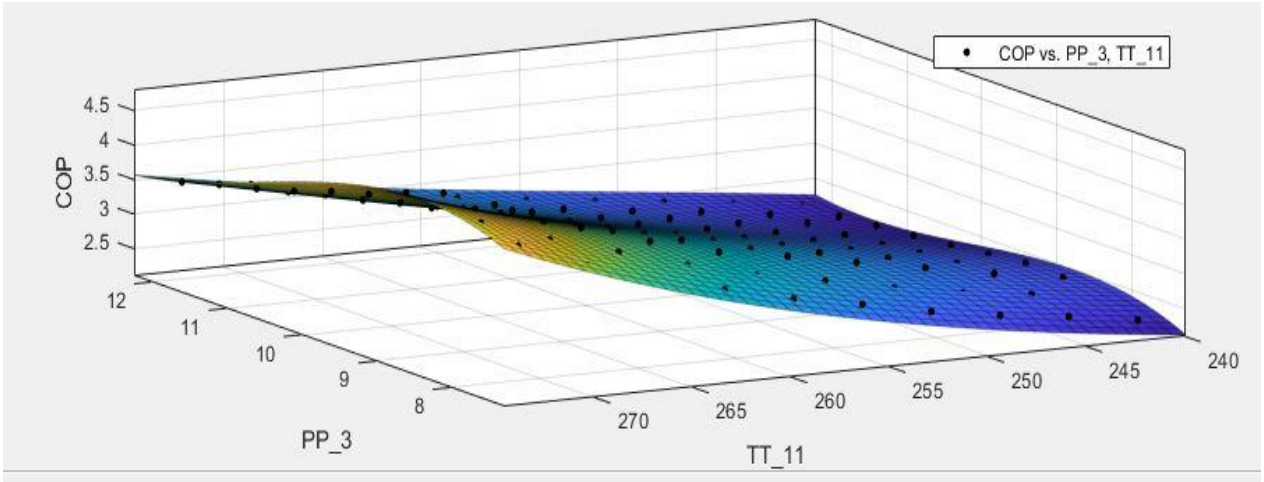

Figure 56- Lineer Regression Analysis of ETC Cycle

The correlation obtained depending on the two parameters examined is shown below:

$$COP = -66.38 - (7.421\,P_{gc}) + (1.117\,T_{eva}) - (0.6459\,P_{gc}^2) + (0.1147\,P_{gc}\,T_{eva}) - (0.006945\,T_{eva}^2) + (0.02921\,P_{gc}^3) - (0.001013\,P_{gc}^2\,T_{eva}) - (0.0001955\,P_{gc}\,T_{eva}^2) + (0.00001244\,T_{eva}^3)$$

$$R^2 = 0.9978$$

The evaporation temperature ranges from 240K to 270K. In addition, the gas refrigerant pressure (Pgc) is varied from 8MPa to 12MPa in 0.5MPa increments.

It was determined the optimum operating conditions of ETC cycle with optimization studies. As the evaporator temperature increases, the COP of the ETC cycle increases and the optimum COP occurs at the evaporator temperature of 270 K. Besides, the gas cooler pressure, on the other hand, reaches the maximum COP value at approximately 8.55 MPa, and then decreases continuously. According to optimization studies, the optimum operation conditions are the same all cycles such as BTC, ESCVI and ETC.

5.CONCLUSION

It was performed the thermodynamics analysis and optimization studies of different CO_2 heat pumps cycles using EES and MATLAB CoolProp software. It was investigated the effects of evaporator temperature, gas cooler pressure, sub-cooling degree, pressure lift ratio and entrainment ratio on COP. As evaporator temperature is increase, COP was increased for all cycles. When the evaporator temperature was 0°C, the minimum COP value was seen in the BTS cycle with a value of about 3.15, and the maximum COP value was observed in the ETC cycle with a value of 4.20. While the gas cooler pressure ranged from 8 to 11.5 MPa, the COP had an appearance of increasing and decreasing in all systems. The maximum COP was reached in all cycles at a pressure of approximately 8.55 MPa. The maximum COP among all systems was obtained in the ETC cycle with the difference of the two ejector system. In systems with ejectors, COP increased as the degree of subcooling increased. The highest exergy loss was observed in the gas cooler in all cycles because the heat is released from the gas cooler to the environment. In cycles with ejector as gas cooler pressure increase, the pressure lift ratio increased and entrainment ratio decreased. As the ejector efficiency increased for the ESCVI cycle, entrainment ratio remained almost at 0.78 and pressure lift ratio increased by approximately 1.06 to 1.12. When the effect of the ejector on COP is examined, the effect of pressure lift ratio and entrainment ratio on COP shows an increasing and decreasing situation as in the gas cooler pressure. The maximum COP value was reached at approximately 1.08 pressure lift ratio (rp) and 0.79 entrainment ratio (μ) in the ESCVI cycle. In the ETC cycle, as the evaporator temperature increases, the pressure lift ratio (r_p) of both the high and low pressure ejector decreases. The loss in the high-pressure ejector is greater than in the low-pressure ejector. Again, as the evaporator temperature increases, there is a slight decrease in the entrainment ratio of the high pressure ejector and the entrainment ratio of the low pressure ejector increases. As the gas cooler pressure increases in the ETC cycle, the pressure lift ratio of the low pressure ejector increases from approximately 1.050 to 1.082, and the entrainment ratio increases from approximately 0.55 to 0.63. Again, with the increase of the gas cooler pressure, there was almost no change in the pressure lift ratio of the high-pressure ejector. The entrainment was decreased from about 0.78 to 0.70. As a result of the system analysis, it has been seen that the most efficient system is the ETC cycle. It was generated a correlation of COP depending on the gas cooler pressure and the evaporator temperature for ESCVI and ETC cycles as a result of the optimization study in MATLAB. A numerical model has been developed to calculate the system performance under different operating conditions for companies planning to produce heat pumps with CO_2 fluid.

6.REFERENCES

[1] Yalçın A. Z., Küresel Çevre Politikalarının Küresel Kamusal Mallar Perspektifinden Değerlendirilmesi, Balıkesir Üniversitesi Sosyal Bilimler Enstitüsü Dergisi, Cilt 12, Sayı 21, Ss.288-309, Haziran 2009

[2] Bulgurcu, H., Kon, O., İlten, N., ―Soğutucu Akışkanların Çevresel Etkileri İle İlgili Yeni Yasal Düzenlemeler Ve Hedefler ―, VIII. Ulusal Tesisat Mühendisliği Kongresi, 2007

[3] Özkol, N.; ―Uygulamalı Soğutma Tekniği, TMMOB Makine Mühendisleri Odası Yayın No: 115, Nisan 1999, Ankara.

[4] 2006 ASHRAE Handbook-Refrigeration (SI)

[5] PEARSON A., Carbon dioxide—new uses for an old refrigerant, 2005

[6] Jørn Stene, (February 2004), Residential CO_2 Heat Pump System for Combined Space Heating and Hot Water Heating, EPT Report 2004:6

[7] Supriya Dharkar, (2015) CO_2 Heat Pumps For Commercial Building Applications With Simultaneous Heating And Cooling Demand, A Thesis Submitted to the Faculty of Purdue University

[8] Arif Emre Özgür, Ahmet Kabul, Hilmi Cenk Bayrakçı, (2015) CO_2 Akışkanlı Isı Pompası Sistemlerinin Mahal Isıtma Amaçlı Kullanımı, 12. Ulusal Tesisat Mühendisliği Kongresi – 8-11 Nisan 2015/İzmir, 863

[9] Venkata Satish Duddumpudi-2010 Transcritical CO_2 Air Source Heat Pump for Average UK Domestic Housing with High Temperature Hydronic Heat Distribution System, University of Strathclyde Engineering Thesis

[10] Ahmed Bensafi, Bernard Thonon,(October 2007), Transcritical R744(CO_2) Heat Pumps Technician's Manual, Sherhpa Project[8]

[11] Thermophysical Properties R744, International Institute of Refrigeration, 2003 [7]

[12] IIR 15th Informatory Note on Refrigerants, February 2000 [8]

[13] Tews, Martin, CO_2 Heat Pumps: Operating Principle And Areas Of Application," https://www.engie-refrigeration.de/en/magazine/CO_2-heat-pumps-operating-principle-and-areas-application 18 July 2019 "

[14] Nishad Dharam Raj, Mirza Shujathullah, Melapundi Dinesh, Patlola Varun Reddy, Oct.-2016, Thermodynamic Analysis Of Gas Compressor, International Journal Of Mechanical And Production Engineering, Issn: 2320-2092, Volume- 4, Issue-10, Oct.-2016

[15] Çengel Yunus A., Boles Michael A., Thermodyanmics An Engineering Approach, Fifth Edition, 239

[16] Çengel Yunus A., Heat Transfer A Practical Approach, Second Edition, 690-691

[17] X.Fang , (June 1999) Modeling and Analysis of Gas Coolers, Air Conditioning and Refrigeration Center, University of Illinois,Mechanical & Industrial Engineering Dept. ,ACRC CR-16

[18] Baris Yilmaz, Ebru Mancuhan, Nasuh Erdonmez, (2018) A Parametric Study on a Subcritical CO_2/NH3 Cascade Refrigeration System for Low Temperature Applications, Journal of Energy Resources Technology, Vol. 140, 092004-1

[19] O. Joneydi Shariatzadeh, S.S. Abolhassani, M. Rahmani, M. Ziaee Nejad, (2016) Comparison Of Transcritical CO_2 Refrigeration Cycle With Expander And Throttling Valve Including/Excluding Internal Heat Exchanger: Exergy And Energy Points Of View, Applied Thermal Engineering, 93, 779–787

[20] EES, 2017, “Engineering Equation Solver,” Academic Commercial V10.326, fChart Software Inc., Madison, WI.

[21] Bell, Ian H. and Wronski, Jorrit and Quoilin, Sylvain and Lemort, Vincent, (2014), Pure and Pseudo-pure Fluid Thermophysical Property Evaluation and the Open-Source Thermophysical Property Library CoolProp, Industrial \& Engineering Chemistry Research, 53,6, 2498-2508